# Understanding Deep Learning Errata

February 8, 2026

Much gratitude to everyone who has pointed out mistakes. If you find a problem not listed here, please contact me via github or by mailing me at udlbookmail@gmail.com.

# Instructions

To find which errata are relevant to your version of the book, first consult the copyright page at the start of the book just before the dedication. The printing will be stated (e.g., "Second printing") just before the line that says "Library of Congress...". If it doesn't specify the printing here, then you have the first printing.

This document is organized by printing. If you have the first printing of the book, all errata are relevant to you. If you have the second printing, then only the errata in the sections for second and third printings are relevant. If you have the third printing, then only the errata for the third printing is relevant and so on.

At the time of writing, the most recent printing is the $5^{th}$. If you are worried about purchasing the book in the light of this evolving document, please feel reassured that the last couple of printings have had very few true errata. Most of the changes described in this document are very minor.

# Errors

These are things that might genuinely confuse you. There is a list of more minor changes (e.g., math symbols that are in bold but should not be, missing brackets, slight rephrasings, changing tiny things for consistency with other chapters) at the end of this document.

## Fifth printing (Jan 2025)

- Chapter 8 Notes. ~~This approach is known as cross-validation~~ . It turns out I was wrong about this. It's only called cross-validation when you split the data into train/test/validation in multiple ways and combine results.
- Section 15.2.2: In the previous section, we saw that when the discriminator is optimal, the loss function ~~minimizes~~ maximizes a measure of the distance between the generated and real samples.
- Problem 19.8: Brackets were in the wrong place in the answer. I have also made a few other improvements for clarity and added a hint. New question:

  The estimate of the gradient in equation 19.34 can be written as:

$$\mathbb{E}_{\boldsymbol{\tau}}\Big[\mathrm{g}[\boldsymbol{\theta}](r[\boldsymbol{\tau}_t]-b)\Big],$$

  where

$$\mathrm{g}[\boldsymbol{\theta},\tau] = \sum_{t=1}^{T}\frac{\partial \log\big[Pr(a_t|\mathbf{s}_t,\boldsymbol{\theta})]\big]}{\partial\boldsymbol{\theta}},$$

  and

$$r[\boldsymbol{\tau}] = \sum_{k=t}^{T} r_k.$$

Show that the value of $b$ that minimizes the variance of the gradient estimate is given by:

$$b = \frac{\mathbb{E}\left[\mathrm{g}[\boldsymbol{\theta}, \boldsymbol{\tau}]^2 r[\boldsymbol{\tau}]\right]}{\mathbb{E}\left[\mathrm{g}[\boldsymbol{\theta}, \boldsymbol{\tau}]^2\right]}.$$

You will need to use the result from equation 19.35.

- Appendix B.3.7 – Rewritten as confused singular values and eigenvalues: If we multiply the set of 2D points on a unit circle by a $2 \times 2$ matrix $\mathbf{A}$, they map to an ellipse (figure **??**). The radii of the major and minor axes of this ellipse (i.e., the longest and shortest directions) correspond to the magnitude of the ~~*eigenvalues*~~ *singular values* $\lambda_1$ and $\lambda_2$ of the matrix. ~~The eigenvalues also have a sign, which relates to whether the matrix reflects the inputs about the origin.~~ The same idea applies in higher dimensions. A $D-$dimensional spheroid is mapped by a $D \times D$ matrix $\mathbf{A}$ to a $D$-dimensional ellipsoid. The radii of the $D$ principal axes of this ellipsoid determine the magnitude of the ~~eigenvalues~~ singular values. For symmetric square matrices, the same information is captured by the *eigenvalues* which are here the same as the singular values .

## Fourth printing (Jun 2024)

There have been only seven errors reported since February 2024 when the second printing was submitted. The book is very stable, so don't be put off from buying a physical copy.

- Figure 12.7 (and legend): Changed to reflect the fact that LayerNorm is applied separately to each embedding. See figure 1.1 of this document. Text in Section 12.4 changed to "This is similar to BatchNorm but normalizes each embedding in each batch element separately using statistics calculated across its D embedding dimensions."

- Figure 14.5: The precision can be computed as the proportion of ~~real examples~~ samples that lie within the approximated manifold of ~~samples~~ real examples . Similarly, the recall is computed as the proportion of ~~real examples~~ samples that lie within the approximated manifold of ~~samples~~ real examples (not shown).

- Problem 15.1: What will the loss be in equation 15.9 when $Pr(\mathbf{x}^*) = Pr(\mathbf{x})$?

- Section 16.3.1 This can be inverted in $\mathcal{O}[D^2]$, and the log determinant is just the sum of the log of the absolute values on the diagonals of **L** and **D**

- Section 16.3.2 (and similar changes in problem 16.9). A simple example is a piecewise linear function with $K$ regions (figure 16.5) which maps $[0, 1]$ to $[0, 1]$ as:

$$\mathrm{f}[h, \boldsymbol{\phi}] = \left(\sum_{k=1}^{b-1} \phi_k\right) + (hK - b + 1)\phi_b, \tag{1.1}$$

where the parameters $\phi_1, \phi_2, \ldots, \phi_K$ are positive and sum to 1, and $b = \lfloor Kh \rfloor + 1$ is the index of the bin that contains $h$.

- Equation 16.22:

$$\begin{aligned} \log\left[\left|\mathbf{I} + \frac{\partial \mathbf{f}[\mathbf{h}, \boldsymbol{\phi}]}{\partial \mathbf{h}}\right|\right] &= \mathrm{trace}\left[\log\left[\mathbf{I} + \frac{\partial \mathbf{f}[\mathbf{h}, \boldsymbol{\phi}]}{\partial \mathbf{h}}\right]\right] \\ &= \sum_{k=1}^{\infty} \frac{(-1)^{k-1}}{k} \mathrm{trace}\left[\frac{\partial \mathbf{f}[\mathbf{h}, \boldsymbol{\phi}]}{\partial \mathbf{h}}\right]^k, \end{aligned}$$

- Section 16.3.7: Assuming that the slope of the activation functions is not greater than one, this is equivalent to ensuring the largest ~~eigenvalue~~ singular value of each weight matrix $\boldsymbol{\Omega}$ must be less than one.

- Appendix B.1 Definition of surjection was wrong. Should be: A *surjection* is a function where every element in the second set receives a mapping from the first (but there may be multiple elements of the first set that are mapped to the same element of the second set).

## Second and third printings (Mar. 2024)

The book was reprinted twice around March 2024.

- Equation 6.12

$$\begin{aligned} \mathbf{m}_{t+1} &\leftarrow \beta \cdot \mathbf{m}_t + (1-\beta) \sum_{i \in \mathcal{B}_t} \frac{\partial \ell_i[\boldsymbol{\phi}_t - \alpha\beta \cdot \mathbf{m}_t]}{\partial \boldsymbol{\phi}} \\ \boldsymbol{\phi}_{t+1} &\leftarrow \boldsymbol{\phi}_t - \alpha \cdot \mathbf{m}_{t+1}, \end{aligned} \tag{1.2}$$

- Equation 6.18:

$$\begin{aligned} \mathbf{m}_{t+1} &\leftarrow \beta \cdot \mathbf{m}_t + (1-\beta) \sum_{i \in \mathcal{B}_t} \frac{\partial \ell_i[\boldsymbol{\phi}_t]}{\partial \boldsymbol{\phi}} \\ \mathbf{v}_{t+1} &\leftarrow \gamma \cdot \mathbf{v}_t + (1-\gamma) \left(\sum_{i \in \mathcal{B}_t} \frac{\partial \ell_i[\boldsymbol{\phi}_t]}{\partial \boldsymbol{\phi}}\right)^2, \end{aligned} \tag{1.3}$$

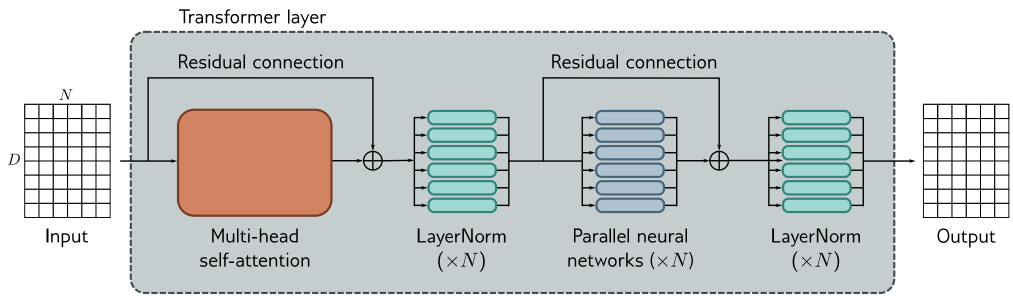


**Figure 1.1** Corrected version of figure 12.7. Transformer layer. The input consists of a $D \times N$ matrix containing the $D$-dimensional word embeddings for each of the $N$ input tokens. The output is a matrix of the same size. The transformer layer consists of a series of operations. First, there is a multi-head attention block, allowing the word embeddings to interact with one another. This forms the processing of a residual block, so the inputs are added back to the output. Second, a LayerNorm operation is applied separately to each embedding. Third, there is a second residual layer where the same fully connected neural network is applied separately to each of the $N$ word representations (columns). Finally, LayerNorm is applied again.

- Equation 15.6

$$\begin{aligned} L[\boldsymbol{\phi}] &= -\frac{1}{J}\sum_{j=1}^{J}\left(\log\left[1-\text{sig}[\text{f}[\mathbf{x}_j^*,\boldsymbol{\phi}]]\right]\right)-\frac{1}{I}\sum_{i=1}^{I}\left(\log\left[\text{sig}[\text{f}[\mathbf{x}_i,\boldsymbol{\phi}]]\right]\right) \\ &\approx -\mathbb{E}_{\mathbf{x}^*}\left[\log\left[1-\text{sig}[\text{f}[\mathbf{x}^*,\boldsymbol{\phi}]]\right]\right]-\mathbb{E}_{\mathbf{x}}\left[\log\left[\text{sig}[\text{f}[\mathbf{x},\boldsymbol{\phi}]]\right]\right] \\ &= -\int Pr(\mathbf{x}^*)\log\left[1-\text{sig}[\text{f}[\mathbf{x}^*,\boldsymbol{\phi}]]\right]d\mathbf{x}^*-\int Pr(\mathbf{x})\log\left[\text{sig}[\text{f}[\mathbf{x},\boldsymbol{\phi}]]\right]d\mathbf{x}, \end{aligned} \tag{1.4}$$

- Equation 15.8

$$\begin{aligned} L[\boldsymbol{\phi}] &= -\int Pr(\mathbf{x}^*)\log\left[1-\text{sig}[\text{f}[\mathbf{x}^*,\boldsymbol{\phi}]]\right]d\mathbf{x}^*-\int Pr(\mathbf{x})\log\left[\text{sig}[\text{f}[\mathbf{x},\boldsymbol{\phi}]]\right]d\mathbf{x} \\ &= -\int Pr(\mathbf{x}^*)\log\left[1-\frac{Pr(\mathbf{x})}{Pr(\mathbf{x}^*)+Pr(\mathbf{x})}\right]d\mathbf{x}^*-\int Pr(\mathbf{x})\log\left[\frac{Pr(\mathbf{x})}{Pr(\mathbf{x}^*)+Pr(\mathbf{x})}\right]d\mathbf{x} \\ &= -\int Pr(\mathbf{x}^*)\log\left[\frac{Pr(\mathbf{x}^*)}{Pr(\mathbf{x}^*)+Pr(\mathbf{x})}\right]d\mathbf{x}^*-\int Pr(\mathbf{x})\log\left[\frac{Pr(\mathbf{x})}{Pr(\mathbf{x}^*)+Pr(\mathbf{x})}\right]d\mathbf{x}. \end{aligned} \tag{1.5}$$

- Equation 19.40:

$$r[\boldsymbol{\tau}_{it}] \approx r_{it} + \gamma \cdot v[\mathbf{s}_{i,t+1}, \boldsymbol{\phi}].$$

- Section B.3.6: Definition of nullspace was ambiguous/wrong. Last line of this section changed to: Conversely, for a landscape matrix $\mathbf{A}$, the part of the input space that maps to zero (i.e., those $\mathbf{x}$ where $\mathbf{A}\mathbf{x} = \mathbf{0}$) is termed the *nullspace* of the matrix.

- Section C.5.3: The definition of the Fréchet distance was incorrect. Changed to:

$$D_{Fr}\Big[p(x)\big|\big|q(y)\Big] = \sqrt{\min_{\pi(x,y)}\left[\iint \pi(x,y)|x-y|^2 dxdy\right]}, \tag{1.6}$$

where $\pi(x,y)$ represents the set of joint distributions that are compatible with the marginal distributions $p(x)$ and $q(y)$. The Fréchet distance can also be formulated as a measure of the maximum distance between the cumulative probability curves.

- Equation C.32:

$$D_{KL}\Big[\text{Norm}[\boldsymbol{\mu}_1, \boldsymbol{\Sigma}_1]\Big|\Big|\text{Norm}[\boldsymbol{\mu}_2, \boldsymbol{\Sigma}_2]\Big] = \frac{1}{2}\left(\log\left[\frac{|\boldsymbol{\Sigma}_2|}{|\boldsymbol{\Sigma}_1|}\right] - D + \text{tr}\left[\boldsymbol{\Sigma}_2^{-1}\boldsymbol{\Sigma}_1\right] + (\boldsymbol{\mu}_2 - \boldsymbol{\mu}_1)\boldsymbol{\Sigma}_2^{-1}(\boldsymbol{\mu}_2 - \boldsymbol{\mu}_1)\right). \tag{1.7}$$

## First printing (Dec. 2023)

These are things that might genuinely confuse you:

- Figure 4.7b had the wrong calculated numbers in it (but pattern is same). Correct version is in figure 1.2 of this document.
- Section 6.3.1 where now the gradients are evaluated at $\boldsymbol{\phi}_t - \alpha\beta \cdot \mathbf{m}_t$.
- Section 7.5.1 The expectation (mean) $\mathbb{E}[f_i{}']$ of the intermediate values $f_i{}'$ is:
- Equation 15.7 The optimal discriminator for an example $\tilde{\mathbf{x}}$ depends on the underlying probabilities:

$$Pr(\text{real}|\tilde{\mathbf{x}}) = \text{sig}\big[\text{f}[\tilde{\mathbf{x}}, \boldsymbol{\phi}]\big] = \frac{Pr(\tilde{\mathbf{x}}|\text{real})}{Pr(\tilde{\mathbf{x}}|\text{generated}) + Pr(\tilde{\mathbf{x}}|\text{real})} = \frac{Pr(\mathbf{x})}{Pr(\mathbf{x}^*) + Pr(\mathbf{x})}. \tag{1.8}$$

where on the right hand side, we evaluate $\tilde{\mathbf{x}}$ against the generated distribution $Pr(\mathbf{x}^*)$ and the real distribution $Pr(\mathbf{x})$.

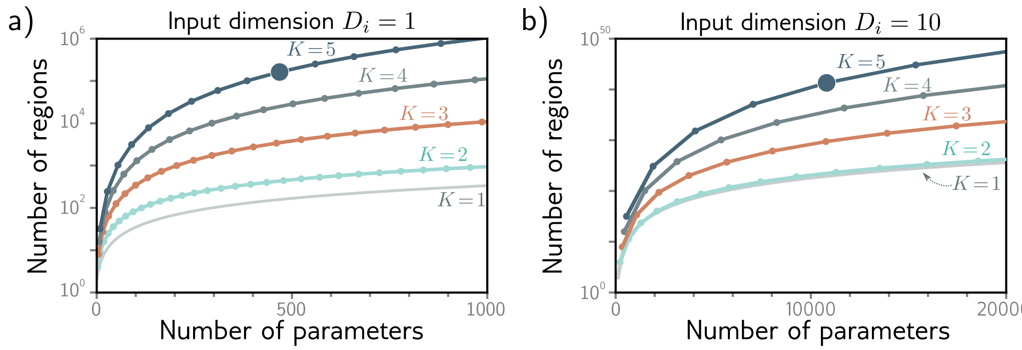


**Figure 1.2** Corrected version of figure 4.7: The maximum number of linear regions for neural networks increases rapidly with the network depth. a) Network with $D_i = 1$ input. Each curve represents a fixed number of hidden layers $K$, as we vary the number of hidden units $D$ per layer. For a fixed parameter budget (horizontal position), deeper networks produce more linear regions than shallower ones. A network with $K = 5$ layers and $D = 10$ hidden units per layer has 471 parameters (highlighted point) and can produce 161,051 regions. b) Network with $D_i = 10$ inputs. Each subsequent point along a curve represents ten hidden units. Here, a model with $K = 5$ layers and $D = 50$ hidden units per layer has 10,801 parameters (highlighted point) and can create more than $10^{40}$ linear regions.

- Equation 15.9. First integrand should be with respect to $\mathbf{x}^*$. Correct version is:

$$\begin{aligned} D_{JS}\Big[Pr(\mathbf{x}^*)\,||\,\,Pr(\mathbf{x})\Big] &= \frac{1}{2}D_{KL}\left[Pr(\mathbf{x}^*)\,\middle|\middle|\,\frac{Pr(\mathbf{x}^*)+Pr(\mathbf{x})}{2}\right] + \frac{1}{2}D_{KL}\left[Pr(\mathbf{x})\,\middle|\middle|\,\frac{Pr(\mathbf{x}^*)+Pr(\mathbf{x})}{2}\right] \\ &= \underbrace{\frac{1}{2}\int Pr(\mathbf{x}^*)\log\left[\frac{2Pr(\mathbf{x}^*)}{Pr(\mathbf{x}^*)+Pr(\mathbf{x})}\right]d\mathbf{x}^*}_{\text{quality}} + \underbrace{\frac{1}{2}\int Pr(\mathbf{x})\log\left[\frac{2Pr(\mathbf{x})}{Pr(\mathbf{x}^*)+Pr(\mathbf{x})}\right]d\mathbf{x}}_{\text{coverage}}. \end{aligned}$$

- Equation 15.12.

$$D_w\Big[Pr(x)||q(x)\Big] = \max_{\mathbf{f}}\left[\sum_i Pr(x=i)f_i - \sum_j q(x=j)f_j\right], \tag{1.9}$$

- Section 15.2.4 Consider distributions $Pr(x = i)$ and $q(x = j)$ defined over $K$ bins. Assume there is a cost $C_{ij}$ associated with moving one unit of mass from bin $i$ in the first distribution to bin $j$ in the second;

- Equation 15.14. Missing bracket and we don't need to use $\mathbf{x}^*$ notation here. Correct version is:

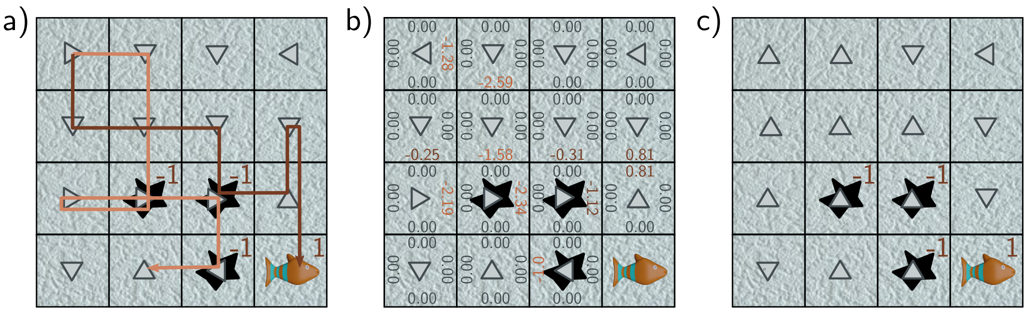


**Figure 1.3** Corrected version of figure 19.11

$$D_w\Big[Pr(\mathbf{x}), q(\mathbf{x})\Big] = \min_{\pi[\bullet,\bullet]}\left[\int\int \pi(\mathbf{x}_1,\mathbf{x}_2)\cdot||\mathbf{x}_1-\mathbf{x}_2||d\mathbf{x}_1 d\mathbf{x}_2\right].$$

- Equation 15.15. Don't need to use $\mathbf{x}^*$ notation here, and second term on right hand side should have $q[\mathbf{x}]$ term not $Pr(\mathbf{x})$. Correct version is:

$$D_w\Big[Pr(\mathbf{x}), q(\mathbf{x})\Big] = \max_{\mathrm{f}[\mathbf{x}]}\left[\int Pr(\mathbf{x})\mathrm{f}[\mathbf{x}]d\mathbf{x} - \int q(\mathbf{x})\mathrm{f}[\mathbf{x}]d\mathbf{x}\right].$$

- Equation 16.12 has a mistake in the second term. It should be:

$$\mathrm{f}[h_d,\boldsymbol{\phi}] = \left(\sum_{k=1}^{b-1}\phi_k\right) + (hK-b)\phi_b.$$

- Equation 17.34.

$$\begin{aligned}\frac{\partial}{\partial\boldsymbol{\phi}}\mathbb{E}_{Pr(x|\boldsymbol{\phi})}\big[\mathrm{f}[x]\big] &= \mathbb{E}_{Pr(x|\boldsymbol{\phi})}\left[\mathrm{f}[x]\frac{\partial}{\partial\boldsymbol{\phi}}\log\big[Pr(x|\boldsymbol{\phi})\big]\right]\\ &\approx \frac{1}{I}\sum_{i=1}^{I}\mathrm{f}[x_i]\frac{\partial}{\partial\boldsymbol{\phi}}\log\big[Pr(x_i|\boldsymbol{\phi})\big].\end{aligned}$$

- Figure 19.11 is wrong in that only the state-action values corresponding to the current state-action pair should be moderated. Correct version above.

- Equation B.4. Square root sign should cover $x$. Correct version is:

$$x! \approx \sqrt{2\pi x}\left(\frac{x}{e}\right)^x.$$

- Appendix B.3.6. Consider a matrix $\mathbf{A}\in\mathbb{R}^{D_1\times D_2}$. If the number of columns $D_2$ of the matrix is fewer than the number of rows $D_1$ (i.e., the matrix is "portrait"),

- Equation C.20. Erroneous minus sign on covariance matrix. Correct version is:

$$\mathbf{x} = \boldsymbol{\mu} + \boldsymbol{\Sigma}^{1/2}\mathbf{z}.$$

# Minor fixes

These are mostly tiny changes that almost certainly won't affect your understanding (e.g., math symbols that are in bold but should not be, missing brackets, slight re-phrasings, changing tiny things for consistency with other chapters). You probably won't even notice them, and most people wouldn't bother making this type of change once the book was already published. I'm mainly listing them to stop people submitting duplicates, and to help translators.

## Fifth printing (Mar 2025)

- Chapter 2 introduction: Slight tweak to language to prevent repeated use of the word "equation": The model is just a mathematical function (i.e., an equation); when the inputs are passed through this ~~equation~~ function , it computes the output, and this is termed *inference*

- Figure 5.1 Caption. Slight rewording: The loss function aims to maximize the probability... $\longrightarrow$ Minimizing the loss function corresponds to maximizing the probability...

- Section 5.12. Minor change to wording to reflect the fact that technically these are not identically distributed since the parameters differ: First, we assume that ~~the data are identically distributed (~~ the form of the probability distribution over the outputs $\mathbf{y}_i$ is the same for each data point. ~~)~~.

- Section 5.12. Removed statement about being i.i.d. at bottom of page 58 as this is technically only true for the errors and even this interpretation only makes sense for continuous distributions.

- Problem 2.3 Changed parameters from $\phi$ to $\phi'$ to indicate that these are not the same parameters as in the discriminative model

- Section 3.4. No need to introduce notation $\mathbf{h}$. using $\mathbf{h} \in \mathbb{R}^D$ hidden units$\rightarrow$ using $D$ hidden units.

- Chapter 3 notes on Universal approximation function. First sentence tweaked to make it more precise. New version: The *width version* of this theorem states that for any continuous function on a compact subset of $\mathbb{R}^n$ and for an arbitrary specified accuracy, there exists a network with one hidden layer containing a finite number of hidden units that can approximate the given function to that accuracy.

- Problem 3.13 What is the activation pattern for each of the seven regions in figure 3.8j?

- Problem 3.16 Write out the equations for a shallow network with two inputs

- Chapter 4 notes on Universal approximation function. Text changed to make it more precise. New text: there exists an approximating for any given continuous function on a compact subset of $\mathbb{R}^{D_i}$ and for an arbitrary specified accuracy. lu2017expressive proved that for any $D_i$-dimensional Lebesgue integrable function and for an arbitrary accuracy, if enough hidden layers are available, then there exists a network with ReLU activation functions and at least $D_i + 4$ hidden units in each layer that can approximate the given function to the given accuracy. This is known as the *depth version* of the universal approximation theorem.

- Section 5.3 We select the univariate normal distribution (figure 5.3)

- Section 5.3.2 For the univariate normal distribution, the

- Figure 5.11 The range of the Poisson distribution should have had curly brackets not square and should be $\{0, 1, 2, 3, \ldots\}$

- Figure 6.6 legend. For this batch, the algorithm moves *downhill* with respect to the batch loss function but in the locally *uphill* direction with respect to the global loss function in panel

- Problem 6.2. Added qualification that must have at least two different samples for matrix to be convex: Prove that this function is convex when there are at least two different samples $x_i$ by showing that the eigenvalues are always positive.

- Section 7.5.1 Slight improvement in notation to remove subscript in some variance terms: $\sigma^2_{f_j} \rightarrow \sigma^2_{f}$ and $\sigma^2_{f'_i} \rightarrow \sigma^2_{f'}$ . Subscript added to left hand side of equation 7.30.

- Problem 7.11: Slight rephrasing of question to make it slightly clearer. New version: Consider training a network with fifty layers using gradient checkpointing. Assume that we store the pre-activations at every tenth hidden layer during the forward pass. Explain how to compute the derivatives in this situation.

- Section 8.4.1 Even with this coarse quantization, there will only be one data point in every ~~$10^{35}$~~ $10^{36}$ bins!

- Section 8.4.1 Minor change in wording to reflect the fact that extrapolation vs. interpolation is a very hazy concept in high dimensions: The tendency of a model to prioritize one solution over another ~~as it extrapolates~~ between data points is known as its *inductive bias*.

- Section 9.1 For consistency, the model $\text{f}[\mathbf{x}, \boldsymbol{\phi}]$ should return a vector and be written as $\mathbf{f}[\mathbf{x}, \boldsymbol{\phi}]$ (two instances of this).

- Equation 9.4 Moved prior to front to emphasize that it is not part of the product.

$$\hat{\boldsymbol{\phi}} = \underset{\boldsymbol{\phi}}{\operatorname{argmax}} \left[ Pr(\boldsymbol{\phi}) \prod_{i=1}^{I} Pr(\mathbf{y}_i | \mathbf{x}_i, \boldsymbol{\phi}) \right]. \tag{1.10}$$

- Problem 9.3 Changed final question to: Derive an expression for the expected loss. (easier but just as illuminating).

- Chapter 9 Notes, self-supervised learning. Missing period before refernece Devlin et al.

- Changed to more specific description of dilation rate: The number of zeros we intersperse between the weights determines the *dilation rate*⟶ The *dilation rate* is the number of zeros interspersed between the weights plus one.

- Section 11.1.1 Slight rephrasing. One conjecture is that ~~at~~ right after initialization, the loss gradients change unpredictably when we modify parameters in early network layers.

- Section 11.4.1. Added qualification to argument as footnote: Technically, this is only true if the BatchNorm operation is applied directly after the network layer. The situation is somewhat more complex if residual paths converge and re-divide between the network layer and the normalization as in figure 11.6c. However, the spirit of the argument remains unchanged.

- Figure 11.14 Legend. Ghost BatchNorm ⟶ Ghost batch normalization

- Figure 12.2 Legend. Self-attention for $N=3$ inputs $\mathbf{x}_n$, each with dimension $D=4$. a) Each input $\mathbf{x}_m$ is operated on independently by the same weights $\boldsymbol{\Omega}_v$ (same color equals same weight) and biases $\boldsymbol{\beta}_v$ (not shown) to form the values $\boldsymbol{\beta}_v + \boldsymbol{\Omega}_v \mathbf{x}_m$.

- Section 12.2 This was ~~less~~ worse than convolutional architectures of the time

- Figure 12.8d legend. After ~~22~~ 23 iterations, the tokens consist of a mix of letters, word fragments, and commonly occurring words.

- Section 12.9 Change of word for clarity. One way to speed up this process is to allow ~~select~~ certain tokens (perhaps at the start of every sentence) to attend to all other tokens (encoder model) or all previous tokens (decoder model).

- Section 13.7.1 The receptive field ~~region~~ is termed the *k-hop neighborhood*.

- Section 15.2.2 If the probability distributions are completely disjoint, this distance is ~~infinite~~ maximal ,

- Section 15.5.1. A few changes to first paragraph to clarify: The Pix2Pix model (figure 15.16) is a network $\hat{\mathbf{x}} = \mathbf{g}[\mathbf{c}, \boldsymbol{\theta}]$ that maps one image $\mathbf{c}$ to a different style image $\mathbf{x}$ using a U-Net (figure 11.10) with parameters $\boldsymbol{\theta}$. A typical use case would be colorization, where the input $\mathbf{c}$ is grayscale, and the output $\mathbf{g}[\mathbf{c}, \boldsymbol{\theta}]$ is color. The output should be similar to the input, and this is encouraged using a *content loss* that penalizes the $\ell_1$ norm $||\mathbf{x} - \mathbf{g}[\mathbf{c}, \boldsymbol{\theta}]||_1$ between the input $\mathbf{c}$ and ground truth output $\mathbf{x}$.

- Problem 15.4. that must be moved and multiply this by the ~~squared~~ distance it must move.

- Problem 15.6. Clarified that variable has standard normal distribution – new version: Consider a latent variable $\mathbf{z} \sim \text{Norm}[\mathbf{0}, \mathbf{I}]$ with dimension 100.

- Section 16.2 Internally consistent within chapter, but changing to be consistent with definition of Jacobian in Chapter 7 and Appendix: The first term is the inverse of the determinant of the $D \times D$ Jacobian matrix $\partial \mathbf{f}[\mathbf{z}, \boldsymbol{\phi}]/\partial \mathbf{z}$, which contains elements $\partial \text{f}_j[\mathbf{z}, \boldsymbol{\phi}]/\partial z_i$ at position $(i, j)$.

- Equation 16.6 - Internally consistent within chapter, but changing to be consistent with definition of Jacobian in Chapter 7 and Appendix:

$$\frac{\partial \mathbf{f}[\mathbf{z}, \boldsymbol{\phi}]}{\partial \mathbf{z}} = \frac{\partial \mathbf{f}_K[\mathbf{f}_{K-1}, \boldsymbol{\phi}_K]}{\partial \mathbf{f}_{K-1}} \cdot \frac{\partial \mathbf{f}_{K-1}[\mathbf{f}_{K-2}, \boldsymbol{\phi}_{K-1}]}{\partial \mathbf{f}_{K-2}} \cdots \frac{\partial \mathbf{f}_2[\mathbf{f}_1, \boldsymbol{\phi}_2]}{\partial \mathbf{f}_1} \cdot \frac{\partial \mathbf{f}_1[\mathbf{z}, \boldsymbol{\phi}_1]}{\partial \mathbf{z}},$$

  becomes:

$$\frac{\partial \mathbf{f}[\mathbf{z}, \boldsymbol{\phi}]}{\partial \mathbf{z}} = \frac{\partial \mathbf{f}_1[\mathbf{z}, \boldsymbol{\phi}_1]}{\partial \mathbf{z}} \cdot \frac{\partial \mathbf{f}_2[\mathbf{f}_1, \boldsymbol{\phi}_2]}{\partial \mathbf{f}_1} \cdots \frac{\partial \mathbf{f}_{K-1}[\mathbf{f}_{K-2}, \boldsymbol{\phi}_{K-1}]}{\partial \mathbf{f}_{K-2}} \cdots \frac{\partial \mathbf{f}_K[\mathbf{f}_{K-1}, \boldsymbol{\phi}_K]}{\partial \mathbf{f}_{K-1}},$$

- Equation 16.7 - Internally consistent within chapter, but changing to be consistent with definition of Jacobian in Chapter 7 and Appendix:

$$\left|\frac{\partial \mathbf{f}[\mathbf{z}, \boldsymbol{\phi}]}{\partial \mathbf{z}}\right| = \left|\frac{\partial \mathbf{f}_K[\mathbf{f}_{K-1}, \boldsymbol{\phi}_K]}{\partial \mathbf{f}_{K-1}}\right| \cdot \left|\frac{\partial \mathbf{f}_{K-1}[\mathbf{f}_{K-2}, \boldsymbol{\phi}_{K-1}]}{\partial \mathbf{f}_{K-2}}\right| \cdots \left|\frac{\partial \mathbf{f}_2[\mathbf{f}_1, \boldsymbol{\phi}_2]}{\partial \mathbf{f}_1}\right| \cdot \left|\frac{\partial \mathbf{f}_1[\mathbf{z}, \boldsymbol{\phi}_1]}{\partial \mathbf{z}}\right|.$$

  becomes:

$$\left|\frac{\partial \mathbf{f}[\mathbf{z}, \boldsymbol{\phi}]}{\partial \mathbf{z}}\right| = \left|\frac{\partial \mathbf{f}_1[\mathbf{z}, \boldsymbol{\phi}_1]}{\partial \mathbf{z}}\right| \cdot \left|\frac{\partial \mathbf{f}_2[\mathbf{f}_1, \boldsymbol{\phi}_2]}{\partial \mathbf{f}_1}\right| \cdots \left|\frac{\partial \mathbf{f}_{K-1}[\mathbf{f}_{K-2}, \boldsymbol{\phi}_{K-1}]}{\partial \mathbf{f}_{K-2}}\right| \cdot \left|\frac{\partial \mathbf{f}_K[\mathbf{f}_{K-1}, \boldsymbol{\phi}_K]}{\partial \mathbf{f}_{K-1}}\right|.$$

- Chapter 17 intro. Slight rewording to avoid ambiguity. Generative adversarial networks learn a mechanism for creating samples that ~~are statistically indistinguishable~~ cannot be distinguished from the training ~~data~~ examples $\{\mathbf{x}_i\}$.

- Figure 17.6 Changed y-axis labels to "log likelihood"

- Section 17.4 The ELBO is *tight* when, for a fixed value of $\boldsymbol{\phi}$, the ELBO and the log likelihood function coincide

- Section 17.8.1 Added explicit probability term for clarity. However, the curse of dimensionality means that almost all values of $\mathbf{z}_n$ that we draw would have a very low probability $Pr(\mathbf{x}|\mathbf{z}_n)$;

- Figure 18.6 Legend: This *is* normally distributed and can be computed in closed form. The first likelihood term $q(z_t^*|z_{t-1})$ is normal in $z_t$

- Equation 18.25. Added expectation with respect to $\mathbf{z}_{t-1}$ in final term of last line

$$\begin{aligned}
&\text{ELBO}\left[\boldsymbol{\phi}_{1\ldots T}\right] \qquad (1.11)\\
&\quad= \int q(\mathbf{z}_{1\ldots T}|\mathbf{x}) \log\left[\frac{Pr(\mathbf{x},\mathbf{z}_{1\ldots T}|\boldsymbol{\phi}_{1\ldots T})}{q(\mathbf{z}_{1\ldots T}|\mathbf{x})}\right] d\mathbf{z}_{1\ldots T}\\
&\quad\approx \int q(\mathbf{z}_{1\ldots T}|\mathbf{x}) \left(\log\left[Pr(\mathbf{x}|\mathbf{z}_1,\boldsymbol{\phi}_1)\right] + \sum_{t=2}^{T}\log\left[\frac{Pr(\mathbf{z}_{t-1}|\mathbf{z}_t,\boldsymbol{\phi}_t)}{q(\mathbf{z}_{t-1}|\mathbf{z}_t,\mathbf{x})}\right]\right) d\mathbf{z}_{1\ldots T}\\
&\quad= \mathbb{E}_{q(\mathbf{z}_1|\mathbf{x})}\Big[\log\left[Pr(\mathbf{x}|\mathbf{z}_1,\boldsymbol{\phi}_1)\right]\Big] - \sum_{t=2}^{T}\mathbb{E}_{q(\mathbf{z}_{t,t-1}|\mathbf{x})}\Big[\mathrm{D}_{KL}\Big[q(\mathbf{z}_{t-1}|\mathbf{z}_t,\mathbf{x})\Big|\Big|Pr(\mathbf{z}_{t-1}|\mathbf{z}_t,\boldsymbol{\phi}_t)\Big]\Big],
\end{aligned}$$

- Figure 19.3. Added state $s_7$ for clarity about when receive reward for fish.

- Figure 19.4 legend. Clarification: Here, the penguin ~~is in state three~~ adoes not know the current state and can only see tiles in the vicinity (dashed box). ~~This~~ Unfortunately, the true state (three) is indistinguishable from what it would see in state nine.

- Section 19.2.2 Edited for consistency of case: Turning this on its head, if we knew the optimal action-values $q^*[s_t, a_t]$, then we ~~can~~ could derive the optimal policy by choosing the action $a_t$ with the highest value

- Section 19.4 Language tweak. We then define a least squares loss based on the consistency of adjacent action values (similar~~ly~~ to the loss in Q-learning, see equation 19.12):

- Section 19.4.1 (further emphasis, that it is the architecture, not the weights that are the same). Using these and other heuristics and with an $\epsilon$-greedy policy, Deep Q-Networks performed at a level comparable to a professional game tester across a set of 49 games using the same network architecture (trained separately for each game).

- Section 19.5.1 Slight tweak to text: ~~The~~ It can be proved that the first term (the rewards before time $t$) does not affect the update from time $t$, so we can write:

- Figure 19.18 shows a single trajectory through an example ~~MRP~~ Markov reward process
- Sectoin 19.5.1 Added extra term to trajectory. Consider a trajectory $\boldsymbol{\tau} = [\mathbf{s}_1, a_1, \mathbf{s}_2, a_2, \ldots, \mathbf{s}_T, a_T, \mathbf{s}$
- Equation 19.24 Equation should end in a comma, not a period.
- Equation 19.32 – minor mistake in indexing, although meaning should be clear

$$r[\boldsymbol{\tau}_{it}] = \sum_{k=t+1}^{T} \gamma^{k-t-1} r_{i,k}, \tag{1.12}$$

- Equations 19.32 and 19.33 – removed factor of $\gamma^t$ from equation 19.33.
- Section 19.5.3. Cleaned up a bit. Policy gradient methods ~~have the drawback that they~~exhibit high variance; many episodes may be needed to get stable ~~updates~~ estimates of the derivatives. One way to reduce this variance is to subtract baseline $b$ from the trajectory returns $r[\boldsymbol{\tau}]$:
- Problem 19.2 Equals sign in equation 19.43 replaced by left-arrow for consistency with earlier parts of the chapter.
- Problem 19.2. Added clarification about notation and removal of misleading math: Show that the value $v[s_t|\pi]$ for the original policy must be less than or equal to $v[s_t|\pi']$ ~~$= q[s_t, \pi'[a|s_t]|\pi]$~~ for the new policy (notation indicates using $\pi'$ for state $s_t$ and $\pi$ thereafter):
- Problem 19.5 Show that this is a contraction mapping (equation ~~16.20~~ 16.30), so that
- Problem 19.6 Added explicit definition of $s$ and $s'$
- Problem 19.7 Clarified that $b$ does not depend on $\tau$.
- Figure 20.1 legend. Slight rephrasing for clarity: "same mean and variance as the original ~~data~~ image dataset.
- Figure 20.8 legend. Added text for clarity. In random Gaussian functions, the number of directions in which the function curves down at points with zero gradient (i.e., saddle points) decreases with the height of the function...
- Section 20.2.5 where the activation function is near-constant, the training gradient is near-zero, so ~~there is no mechanism to improve the model~~ the mechanism to improve the model is extremely weak.
- Section 20.4.2. Slight rephrasing. However, sharpness alone is not a good criterion to predict generalization between datasets; when the labels in the CIFAR dataset are randomized (making generalization impossible), there is no commensurate ~~decrease in the flatness~~ sharpening of the minimum...

- Figure 20.12 legend. Number of parameters was slightly wrong. A fully connected network with two hidden layers, each with 200 units (~~198,450~~ 199,210 parameters)
- Section 20.4.5. Slight rephrasing to improve clarity: the weights are initialized with a variance that is inversely proportional to the width (i.e., with He or Glorot initialization), and the weights ~~change very little from their original values~~ need not change as drastically to fit the data well.
- Section 20.5 Added the word 'test' to make it clear that this is not about training: Indeed, there are almost no examples of state-of-the-art test performance
- Section 20.6.3 Slight rephrasing for improved clarity: that these constraints have a good inductive bias and that it is difficult to ~~force~~ induce shallow networks to obey these constraints
- Section 21.3.4 Year for citation of Keynes changed to 1931
- Section B.3.5 Minor clarification: If we take the inverse of a matrix product $\mathbf{AB}$ where $\mathbf{A}$ and $\mathbf{B}$ are square and invertible, then we can equivalently take the inverse of each matrix individually and reverse the order of multiplication.
- Equation C.37 Equation should end in a comma, not a period.
- Equation C.37 Missing transpose in last term: $(\boldsymbol{\mu}_2 - \boldsymbol{\mu}_1)^T \boldsymbol{\Sigma}_2^{-1}(\boldsymbol{\mu}_2 - \boldsymbol{\mu}_1)$
- Figure B.3. Eigenvalue → singular value
- Appendix B.4.3. Definitions of lower and upper triangular matrices were subtley innacurate. New version: A *lower triangular matrix* has all of its non-zero values on the principal diagonal and/or the positions below this. An *upper* triangular matrix has all of its non-zero values on the principal diagonal and/or the positions above this.
- Appendix B.4.4 It is a special case of an orthogonal matrix, so its inverse is its own transpose, and its determinant is always ~~one~~ $\pm 1$.
- Appendix C.5.3 Changed notation for consistency with equation. The Fréchet distance ~~$D_{FR}$~~$D_{Fr}$ between two distributions $p(x)$ and $q(x)$ is given by

## Fourth printing (Jun 2024)

- Chapter 1 introduction: A *deep neural network* (or *deep network* for short) is a type of machine learning model, and when it is fitted to data, this is referred to as *deep learning*. (+ other minor changes to preserve formatting)
- Chapter 1 introduction: Hence, this chapter also contains a brief primer on AI ethics.

- Section 1.1.2 For the music classification example, the input vector might be of fixed size (perhaps a 10-second clip) but is very high-dimensional (i.e., contains many entries).
- Section 1.1.2 Moreover, ~~structure is naturally two-dimensional~~ it contains spatial structure; two pixels above and below one another are closely related, even if they are not adjacent in the input vector.
- Section 1.2.2 Similarly, real-world images are a tiny subset of the images that can be created by drawing random red, green, and blue (RGB) values for every pixel. (+ other minor changes to preserve formatting)
- Section 1.4 They may ~~contain billions of parameters~~ be enormous, and there is no way we can understand how they work based on examination. (the term parameters is not defined yet)
- Section 1.5 Why do they need ~~so many parameters~~ to be so large? (the term parameters is not defined yet).
- Section 2.1. Added marginal link to appendix for argmin function
- Figure 2.1 legend and three other places in this chapter Removed transpose from parameter vector (unnecessary and confused some people).
- Figure 2.2 Parameters and line in figure 2.2d changed to $\phi_0 = 0.82, \phi_1 = 0.52$ as this gives a slightly lower loss.
- Equation 2.5 Standard $\phi$ on left hand side changed to bold $\boldsymbol{\phi}$.
- Figure 3.5 The symbol $D_i$ is not defined. Added the sentence: This idea generalizes to functions in $D_i$ dimensions.
- Section 4.4.1 Function $\mathbf{f}[\bullet]$ should be bold. New version: A general deep network $\mathbf{y} = \mathbf{f}[\mathbf{x}, \boldsymbol{\phi}]$ with $K$ layers can now be written as
- Figure 4.6 legend: The weights are stored in matrices $\boldsymbol{\Omega}_k$ that ~~pre-~~multiply the activations from the preceding layer.
- Chapter 4 in notes. Lu et al. (2017) proved that there exists a network with ReLU activation functions and at least $D_i + 4$ hidden units in each layer that can approximate any specified $D_i$-dimensional Lebesgue integrable function to arbitrary accuracy given enough layers.
- Chapter 5 introduction: Changed marginal link to ~~Number~~ Sets for consistency with the appendix.
- Section 5.1.1 This shift in perspective raises the question of
- Section 5.2: To perform inference for a new test example $\mathbf{x}$, return either the full distribution $Pr(\mathbf{y}|\mathbf{f}[\mathbf{x}, \hat{\boldsymbol{\phi}}])$ or the value where this distribution is maximized.

- Section 5.3.1: We see that the least squares loss function follows naturally from the assumptions that the predictions are (i) independent and (ii) drawn from a normal distribution with mean $\mu = \mathrm{f}[\mathbf{x}_i, \boldsymbol{\phi}]$.

- Section 5.3.1: We removed the denominator between the third and fourth lines, as this is just a constant positive scaling factor that does not affect the position of the minimum. (other minor changes to preserve formatting)

- Equation 5.12: Inner close square bracket in wrong place

$$\hat{y} = \underset{y}{\mathrm{argmax}} \left[ Pr(y|\mathrm{f}[\mathbf{x}, \hat{\boldsymbol{\phi}}], \sigma^2 \right].$$

- Section 5.3.3 However, there is nothing to stop us from treating $\sigma^2$ as a learned parameter ~~of the model~~and minimizing equation 5.9 with...

- Figure 5.10 legend. ...any vertical slice of this plot produces three values that sum to one

- Section 5.5. Clarity improved by referring to both uses of this notation. where $\mathrm{f}_{y_i}[\mathbf{x}, \boldsymbol{\phi}]$ and $\mathrm{f}_{k'}[\mathbf{x}, \boldsymbol{\phi}]$ denote the $y_i^{th}$ and $k'^{th}$ outputs of the network, respectively.

- Figure 5.12: Model distribution (a normal distribution with parameters $\boldsymbol{\theta} = \{\mu, \sigma^2\}$).

- Figure 5.14: here, two ~~weighted~~ normal distributions, dashed blue and orange curves

- Section 6.1.2 More formally, they are convex, which means that every ~~no~~ chord (line segment between two points on the surface) ~~intersects the function~~ lies above the function and does not intersect it.

- Chapter 6 notes. A function is convex if colorred every ~~no~~ chord (line segment between two points on the surface) ~~intersects the function~~ lies above the function and does not intersect it.

- Chapter 6 notes. However, this is strange since SGD is a special case of Adam (when ~~$\beta = \gamma = 0$~~ $\beta = 0, \gamma = 1$ ) once the modification term (equation 6.16) becomes one, which happens quickly.

- Problem 6.1 A surface is guaranteed to be convex if the eigenvalues of the Hessian $\mathbf{H}[\boldsymbol{\phi}]$ are positive everywhere.

- Equation 7.7 (new label added to unlabelled equation between previous equation 7.6 and 7.7)

- Section 7.4 Now let's consider how the loss changes when the pre-activations $\mathbf{f}_0, \mathbf{f}_1, \mathbf{f}_2$ change.

- Equation 7.26 (formerly, now eq 7.27). Activation should be bolded:

$$\begin{aligned}\mathbf{f}_k &= \boldsymbol{\beta}_k + \boldsymbol{\Omega}_k \mathbf{h}_k \\ &= \boldsymbol{\beta}_k + \boldsymbol{\Omega}_k \mathbf{a}[\mathbf{f}_{k-1}],\end{aligned}$$

- Section 7.5.1 where ~~f~~ **h** represents the ~~pre-~~activations
- Section 7.5.1 where **h** represents the activations, $\boldsymbol{\Omega}$~~,~~ and $\boldsymbol{\beta}$ represent the weights and biases, and $\mathbf{a}[\bullet]$ is the activation function.
- Section 7.5.1 Assuming that the ~~input~~ distribution of pre-activations $f_j$ at the previous layer is symmetric about zero
- Equations 7.29 and 7.30 + nearby text. Added subscript to variance so $\sigma^2_{f'} \rightarrow \sigma^2_{f'_i}$.
- Problem 7.6. Equation number added.
- Section 8.1 This is better than the chance error rate of 90% ~~error rate~~ but far worse than for the training set;
- Section 8.2 To make this easier to visualize, we revert to a 1D ~~linear~~ least squares regression problem
- Section 8.2.2 They combine additively for ~~linear~~ regression tasks with a least squares loss. However, their interaction can be more complex for other types of problems
- Section 8.3 there is nothing we can do to circumvent this, and it represents a fundamental limit on expected model performance
- Section 8.3.3: For a fixed-size training dataset, the variance term typically increases as the model capacity increases.
- Section 8.4.1: Rephrased sentence to avoid potential ambiguity: Second, the test performance continues to improve with capacity even when this exceeds the point where the training data are all classified correctly.
- Figure 8.10. Legend. Training and test ~~loss~~ erroron MNIST-1D... The training and test ~~loss~~ errordecreases to zero... Depending on the loss function, the model, and the amount of noise in the data
- Section 9.1 We seek the parameters $\hat{\boldsymbol{\phi}}$ that minimize ~~minimum of~~ the loss function $L[\boldsymbol{\phi}]$ :
- Section 9.1 where $\mathrm{g}[\boldsymbol{\phi}]$ is a function which ~~that~~ returns a scalar that takes ~~a~~larger values when the parameters are less preferred
- Figure 9.2 legend: L2 regularization in simplified network with 14 hidden units.

- Figure 9.2 legend: For large $\lambda$ (panels e–f), the regularization term overpowers the likelihood term, so the fitted function is too smooth and the overall ~~the fitted function is smoother than the ground truth, so the~~ fit is worse.
- Section 9.2.1: (see notes "Implicit regularization in gradient descent" at end of chapter)
- Section 9.2.2: if the model is over-parameterized, then it may fit all the training data exactly, so each ~~all~~ of these gradient terms will ~~all~~ be zero at the global minimum.
- Section 9.3: We've seen that ~~adding~~ explicit regularization ~~terms~~ encourages the training algorithm to find a good solution by adding extra terms to the loss function.
- Section 9.3.1: The model is trained once, the performance on the validation set is monitored every $T$ iterations, and the associated parameters ~~models~~ are stored. The stored parameters ~~models~~ where the validation performance was best are ~~is~~ selected.
- Section 9.3.3 This makes the network less dependent on any given hidden unit and encourages the weights to have smaller magnitudes so that the change in the function due to the presence or absence of any specific hidden ~~the~~ unit is reduced.
- 9.3.3 *Dropout* ~~randomly~~ clamps a random subset (typically 50%) of hidden units to zero at each iteration of SGD.
- 9.3.3. When several units conspire in this way, eliminating one (as would happen in dropout) causes a considerable change to the output function in ~~that is propagated to~~ the half-space where that unit was active
- Section 9.3.5 The maximum likelihood approach is generally overconfident; ~~in the training phase~~ it selects the most likely parameters during training and uses these to make predictions ~~and bases its predictions on the model defined by these.~~
- Chapter 9 Notes Notably missing from the discussion in this chapter is BatchNorm ~~at~~ and its variants
- Chapter 10 and 11 (multiple places) zero padding $\rightarrow$ zero-padding
- Section 10.2.5 If we only apply a single convolution, information will likely ~~inevitably~~ be lost;
- Section 10.2.5 If the incoming layer has $C_i$ channels and we select a kernel size $K$ per channel, the hidden units in each output channel are computed as a weighted sum over all $C_i$ channels and $K$ kernel entries ~~positions~~ using a weight matrix $\boldsymbol{\Omega} \in \mathbb{R}^{C_i \times K}$ and one bias. Hence, if there are $C_o$ channels in the next layer, then we need $\boldsymbol{\Omega} \in \mathbb{R}^{C_i \times C_o \times K}$ weights and $\boldsymbol{\beta} \in \mathbb{R}^{C_o}$ biases.

- Figure 10.7 legend: The MNIST-1D input has dimension $D_i = 40$. The first convolutional layer has fifteen channels, kernel size three, stride two, and only retains "valid" positions to make a ~~representation~~ hidden layer with nineteen positions and fifteen channels. The following two convolutional layers have the same settings, gradually reducing the representation size at each subsequent hidden layer.
- Section 10.4.3 Combined with a bias and activation function, it is equivalent to running the same fully connected network on the input channels at every position.
- Section 10.6 As ~~the network progresses~~ a data example passes through the network, the spatial dimensions usually decrease by factors of two, and the ~~number of~~ channels increase~~s~~by factors of two.
- Chapter 10 Notes p183. However, the ConvolutionOrthogonal initializer (Xiao et al., 2018a) is specialized for convolutional networks ~~(Xiao et al., 2018a)~~.
- Chapter 10 Notes p184 (Lin et al., 2017b) ~~Lin et al. (2017b)~~, (Redmon et al., 2016) ~~Redmon et al. (2016)~~.
- Problem 10.4 Write out the equation for a 1D convolution with kernel size seven, dilation rate of three, and stride of three. ~~You may assume that the input is padded with zeros at positions $x_{-2}$, $x_{-1}$ and $x_0$~~
- Problem 10.6. Draw a $12\times6$ ~~$6\times12$~~ weight matrix in the style of figure 10.4d relating inputs $x_1, \ldots, x_6$ to outputs $h_1, \ldots, h_{12}$ in the multi-channel convolution as depicted in figures 10.5a–b.
- Problem 10.7. Draw a $6\times12$ ~~$12\times6$~~ weight matrix in the style of figure 10.4d relating inputs $h_1, \ldots, h_{12}$ to outputs $h'_1, \ldots, h'_6$ in the multi-channel convolution in figure 10.5c.
- Problem 10.15 Show that the weight matrix for 1D convolution with kernel size three and stride two is equivalent to composing the matrices for 1D convolution with kernel size three and stride one and this sampling matrix.
- Problem 10.17 What is the receptive field size at each of the first three layers of AlexNet (i.e., the first three orange blocks in figure 10.16)?
- Chapter 11 Introduction: The previous chapter described how image classification performance improved as the depth of convolutional networks was extended from eight layers (AlexNet) to ~~eighteen~~ nineteen layers (VGG).
- Section 11.1.1 In principle, we can add as many layers as we want, and in the previous chapter, we saw that adding more layers to a convolutional network does improve performance; the VGG network (figure 10.17), which has ~~eighteen~~ nineteen layers, outperforms AlexNet (figure 10.16)...
- Section 11.1.1 When we change the parameters that determine $\mathbf{f}_1$, *all* of the derivatives in this sequence ~~can change~~ are evaluated at slightly different locations since layers $\mathbf{f}_2, \mathbf{f}_3$, and $\mathbf{f}_4$ are themselves computed from $\mathbf{f}_1$.

- Section 11.2 Rephrased for clarity. A complementary way of thinking about this residual network is that it creates sixteen paths with differing numbers of transformations between input and output ~~of different lengths from input to output~~.
- Section 11.4.1 Hence, it both creates redundancy in the ~~weight parameters~~ weights and biases and
- Section 11.5.1 Rephrasing of fourth and fifth sentences to emphasize that these changes happen between ResNet blocks. New version: The resolution is decreased between adjacent ResNet blocks using convolutions with stride two. Channels are similarly added by either appending zeros to the representation or applying an extra 1×1 convolution.
- Section 11.5.2 Concatenation across the downsampling makes no sense since the representations have different spatial sizes.
- Chapter 11 Notes p202. A second ReLU function was applied after this block was added back to the main representation. This architecture was termed *ResNet v1*.
- Chapter 11 Notes p203. (networks for processing sequences, in which the previous output is fed back as an additional input as we move through the sequence ~~(~~see figure 12.19)
- Problem 11.2 How many paths of each length would there be ~~if~~ with (i) three residual blocks and (ii) five residual blocks? Deduce the rule for $K$ residual blocks.
- Section 12.2 Rephrasing to avoid potential ambiguity. A self-attention block $\mathbf{sa}[\bullet]$ takes $N$ inputs $\mathbf{x}_1, \ldots, \mathbf{x}_N$, each of dimension $D \times 1$, and returns $N$ ~~output vectors of the same size~~, outputs each of which is also of size $D \times 1$.
- Section 12.2.1 This computation scales linearly with the sequence length $N$, so it needs fewer parameters than a fully connected network relating all $DN$ inputs to all $DN$ ~~outputs. T~~ values. In fact, the value computation can be viewed as a sparse matrix operation with shared parameters that relates these $DN$ quantities (figure 10.2b)
- Figure 12.2 Legend. Each output is a linear combination of the values, with ~~a shared~~ the attention weight a[$\mathbf{x}_m$ ...
- Section 12.3.1 Observant readers will have noticed that the self-attention mechanism ~~discards~~ overlooks important information: the computation ~~is the same regardless~~ does not take into account the order of the inputs $\mathbf{x}_n$.
- Section 12.3.1 Changed word to avoid ambiguity: The input to a self-attention mechanism may be an entire sentence, many sentences, or just a fragment of a sentence, and the absolute position of a word is much less important than the relative position between two ~~inputs~~ words. Figure 12.8. Moved the following sentence from descripton of panel c to the description of panel b to avoid ambiguity: Note that the last character of the first token to be merged cannot be whitespace, which prevents merging across words.

- Section 12.6: i.e., the matrices $\mathbf{\Omega}_{vh}, \mathbf{\Omega}_{qh}, \mathbf{\Omega}_{kh}$ are ~~$1024 \times 64$~~ $64 \times 1024$
- Section 12.6. In the *fine-tuning stage*, the resulting network is adapted to solve a particular task using a smaller body of ~~supervised~~ labelled training data.
- Figure 12.10 legend: Minor rephrasing to improve clarity. As such, the output embeddings are passed through a softmax function, and the multiclass classification loss (section 5.24) is used.→ To this end, the outputs corresponding to the masked tokens are passed through softmax functions, and a multiclass classification loss (section 5.24) is applied to each
- Section 12.7.1 Rephrased to avoid ambiguity: GPT3 ~~constructs~~ is an autoregressive language model.
- Section 12.7.1 Original text is true, but this is a more useful statement given where we are in the text: The autoregressive formulation demonstrates the connection between maximizing the ~~log~~ joint probability of the tokens ~~in the loss function~~ and the next token prediction task
- Section 12.7.1 Slight rephrasing of sentence before equation 12.14. An autoregressive model predicts the conditional distributions $Pr(t_n|t_1, \ldots, t_{n-1})$ of each token given all the prior tokens, and hence indirectly computes the joint probability $Pr(t_1, t_2, \ldots, t_N)$ of all $N$ tokens:
- Section 12.7.2 Added some constructive redundancy: Ideally, we would pass in the whole sentence and compute all the log probabilities and gradients ~~simultaneously~~ in the same forward pass rather than doing a forward pass for each token in the sentence.
- Section 12.7.2 Slight rewording to improve clarity: To train a decoder, we seek parameters that maximize the log probability of the input text under the autoregressive model (i.e., that maximize the sum of the log conditional probability terms).
- Section 12.7.2: Slightly better: Consequently, after the transformer layers, a single linear layer maps each ~~word~~ output embedding to the size of the vocabulary, followed by a **softmax**[•] function that converts these values to probabilities.
- Section 12.7.3: The new extended sequence can be fed back into the decoder network ~~that outputs~~ to yield the probability distribution over the next token.
- Section 12.7.3: For example, *beam search* keeps track of multiple possible sentence completions to find the overall most likely sequence of words (which is not necessarily found by greedily choosing the most likely ~~next~~ word at each step).
- Section 12.8 Improved first two sentences slightly: Translation between languages is an example of a *sequence-to-sequence* task. One common approach uses both an encoder (to compute a good representation of the source sentence) and a decoder (to generate the sentence in the target language). This is aptly called an *encoder-decoder* model.

- Figure 12.14 Legend. The flow of computation is the same as in standard self-attention . However, but the queries are calculated from the decoder embeddings $\mathbf{X}_{dec}$, and the keys and values from the encoder embeddings $\mathbf{X}_{enc}$. In the context of translation For translation tasks, the encoder contains information about the source language statistics, and the decoder contains information about the target language statistics.

- Section 12.10.1 Third paragraph, sentence phrasing changed for improved clarity: Each pixel's final embedding is averaged, and a linear layer maps these values to activations which are passed through a softmax layer to predict class probabilities.

- Section 12.10.2 Fixed minor inaccuracy Each patch is mapped to a lower dimension an input embedding via a learned linear transformation,

- Section 12.10.3. Reworded paragraph to include references to receptive field: The Vision Transformer differs from convolutional architectures in that it operates on a single scale and has a receptive field that covers the whole image. Several transformer models that process the image at multiple scales have been proposed. Similarly to convolutional networks, these generally start with small high resolution patches and few channels and gradually enlarge the receptive field, decrease the spatial resolution and increase the number of channels.

- Figure 12.18 legend. Added clarification about windows: The transformer network applies self-attention to the patches within each window independently (i.e., patches only attend to other patches in the same window).

- Chapter 12 Notes. The *synthesizer* simplifies this idea by simply

- Figure 14.1 Legend. Latent variable models define a mapping between an underlying explanatory (latent) variable and the data. Theyand may fall into any of the above categories.

- Section 14.3. Slightly improvement in clarity to distinguish random variable from its instantiation. Changed all mentions of $Pr(y_i|\mathbf{x}_i^*)$ to $Pr(y|\mathbf{x}_i^*)$.

- Section 15.2.4: It is a *linear programming problem* in its *primal form*:.

- Section 15.2.6: Changed to stop nasty line wrap-over: One way to achieve this is to clip the discriminator weights to a small range (e.g., $\pm 0.01$)

- Figure 15.9: Removed brackets around image sizes for consistency with text.

- Figure 15.11: Changed caption to reflect the fact that multiple tricks have been used to get good performance here, not just progressive growing. New caption: "Combining methods. GANs can generate realistic images of faces when trained on CELEBA-HQ dataset and more complex, variable objects when trained on LSUN categories."

- Section 15.5.3 Added marginal reference to $\ell_1$-norm

- Section 15.6: Figure 15.20 shows examples of manipulating the style and noise vectors ~~are~~ at different scales
- Chapter 15 Notes on Conditional GANS. Images generated by GANs have variously been conditioned on classes (~~e.g.,~~Odena et al., 2017), input text (Reed et al., 2016a; Zhang et al., 2017d), attributes (Yan et al., 2016; Donahue et al., 2018a; Xiao et al., 2018b), bounding boxes and keypoints (Reed et al., 2016b), and images (~~e.g.,~~Isola et al., 2017)~~)~~
- Chapter 15. Notes on Adversarial loss. In many image translation tasks, there is no "generator"; ~~such models~~ these can be considered supervised learning tasks with an adversarial loss that encourages realism.
- Problem 15.2: Write an equation relating the loss $L$ in equation 15.8 to the Jensen-Shannon distance $D_{JS}\left[Pr(\mathbf{x}^*)\,||\,Pr(\mathbf{x})\right]$ in equation 15.9.
- Section 16.3.3: If the function $\mathbf{g}[\bullet, \boldsymbol{\phi}]$ is an elementwise flow, the Jacobian will be lower triangular ~~diagonal~~with the identity matrix in the top-left quadrant and the derivatives of the elementwise transformation in the bottom-right.
- Section 17.1.1 As in equation 17.2, the probability ~~likelihood~~ $Pr(x)$ is given by the marginalization over the latent variable $z$
- Section 17.4.2 This is termed the reconstruction loss → This measures the reconstruction accuracy. (Technically, it's not a loss since we are maximizing it).
- Chapter 17 Notes. Missing period: Other authors have investigated using a discrete latent space (Van Den Oord et al., 2017; Razavi et al., 2019b; Rolfe, 2017; Vahdat et al., 2018a,b).
- Problem 17.7 Derive the EM algorithm for fitting the 1D mixture of Gaussians ~~algorithm~~ model with $N$ components.
- Equation 18.34 Added brackets to equation:

$$L[\boldsymbol{\phi}_{1\ldots T}] = \sum_{i=1}^{I}\Bigg(-\log\Big[\text{Norm}_{\mathbf{x}_i}\left[\mathbf{f}_1[\mathbf{z}_{i1},\boldsymbol{\phi}_1],\sigma_1^2\mathbf{I}\right]\Big] + \sum_{t=2}^{T}\frac{1}{2\sigma_t^2}\left\|\left(\frac{1}{\sqrt{1-\beta_t}}\mathbf{z}_{it} - \frac{\beta_t}{\sqrt{1-\alpha_t}\sqrt{1-\beta_t}}\boldsymbol{\epsilon}_{it}\right) - \mathbf{f}_t[\mathbf{z}_{it},\boldsymbol{\phi}_t]\right\|^2\Bigg).$$

- Under Equation 18.36: Added missing equation number in equation after 18.36.
- Figure 18.10 Caption: ...including the denoising diffusion implicit ~~(DDIM)~~ model (DDIM)
- Chapter 18 notes. One of these models is the denoising diffusion implicit model (DDIM), in which the updates are not stochastic (figure 10.8~~b~~c). This model is amenable to taking larger steps (figure 10.8~~d~~e) without inducing large errors.

- Problem 18.1 Show that if $\text{Cov}[\mathbf{x}_{t-1}] = \mathbf{I}$ and we use the update:

$$\mathbf{x}_t = \sqrt{1-\beta_t}\cdot\mathbf{x}_{t-1} + \sqrt{\beta_t}\cdot\boldsymbol{\epsilon}_t,$$

then $\text{Cov}[\mathbf{x}_t] = \mathbf{I}$, so the variance stays the same.

- Chapter 19 introduction: In finance, an RL algorithm might control a virtual trader (the agent) who buys or sells assets (the actions) on a ~~trading platform~~ financial exchange (the environment) to maximize profit (the reward).

- Section 19.1.5 Minor reprhrasing: The environment then ~~assigns~~ advances to the next state according to $Pr(s_{t+1}|s_t, a_t)$ and issues a reward according to $Pr(r_{t+1}|s_t, a_t)$.

- Figure 19.3 legend. Slight rephrasing to improve clarity: The agent (penguin) can perform one of a set of actions in each state. ~~The action influences both the probability of moving to the successor state and the probability of receiving rewards.~~ b) Here, the four actions correspond to moving up, right, down, and left. c) For any state (here, state 6), the action changes the probability of moving to the next state. The penguin moves in the intended direction with 50% probability, but the ice is slippery, so it may slide to one of the other adjacent positions with equal probability. Accordingly, in panel (a), the action taken (gray arrows) doesn't always line up with the trajectory (orange line). ~~Here,~~ In general, the action can also influence the probability of receiving rewards, but in this example the action does not affect the reward...

- Figure 19.4. Slight rephrasing for clarity: Here, the penguin is in state three and can only see ~~the region in the dashed box~~ tiles in the vicinity (dashed box).

- Section 19.1.3 Rephrase for clarity: An MDP produces a sequence $(s_1, a_1, r_2), (s_2, a_2, r_3), (s_3, a_3, r_4)\ldots$ of states $s_t$, actions $a_t$, and rewards $r_{t+1}$ which are received at the subsequent time-step (figure 19.3).

- Section 19.3. Added footnote for "Model-based methods": The term model refers here to the MDP and not a machine learning model.

- Section 19.3 Reworded to avoid ambiguity. Conversely, model-free methods ~~eschew a model of the MDP and fall into two classes~~ assume that the transition matrix and reward structure of the underlying MDP are unknown. These methods fall into two families:

- Section 19.3.2. Not wrong, but clearer with these tweaks: Each starts with a given state and action and thereafter follows the current policy, producing a series of actions, states, and ~~returns~~ rewards (figure 2.11a). The action value for a given state-action pair under the current policy is estimated as the average of the empirical returns (i.e., cumulative sums of time-discounted rewards) that follow each time this pair occurs (figure 2.11b).

- Figure 19.10b: Tweaked four of the values as had rounded oddly in computation.

- Figure 19.11c: Policy in cell 12 should not be updated (arrow should still point upwards). We have not performed the "down arrow" action, so we can't change this.
- Section 19.3.3 Changed tense for internal consistency: Monte Carlo methods sampled the MDP to acquire information.
- Figure 19.14: Input should be tagged as having size $84 \times 84 \times 4$.
- Section 19.4.2: ...leads to a systematic bias in the estimated action values $q[s_t, a_t]$.
- Equation 19.30: Changed for compatibility with earlier definition of reward:

$$r[\boldsymbol{\tau}_i] = \sum_{t=1}^{T} r_{i,t+1} = \sum_{k=1}^{t} r_{i,k+1} + \sum_{k=t}^{T} r_{i,k+1},$$

- Equation 19.31: Changed for compatibility with earlier definition of reward:

$$\boldsymbol{\theta} \leftarrow \boldsymbol{\theta} + \alpha \cdot \frac{1}{I}\sum_{i=1}^{I}\sum_{t=1}^{T} \frac{\partial \log\bigl[\pi[a_{it}|\mathbf{s}_{it}, \boldsymbol{\theta}]\bigr]}{\partial \boldsymbol{\theta}} \sum_{k=t}^{T} r_{i,k+1}.$$

- Equation 19.32: Changed for compatibility with earlier definition of reward:

$$r[\boldsymbol{\tau}_{it}] = \sum_{k=t+1}^{T} \gamma^{k-t-1} r_{i,k+1},$$

- Section 19.5.3 One way to reduce this variance is to subtract ~~the trajectory returns $r[\boldsymbol{\tau}]$ from a baseline $b$~~ a baseline $b$ from the trajectory returns $r[\boldsymbol{\tau}]$:
- Equation 19.39: Changed for compatibility with earlier definition of reward:

$$L[\boldsymbol{\phi}] = \sum_{i=1}^{I}\sum_{t=1}^{T}\left(v[\mathbf{s}_{it}, \boldsymbol{\phi}] - \sum_{j=t}^{T} r_{i,j+1}\right)^2.$$

- Equation 19.40: Changed for compatibility with earlier definition of reward:

$$r[\boldsymbol{\tau}_{it}] \approx r_{i,t+1} + \gamma \cdot v[\mathbf{s}_{i,t+1}, \boldsymbol{\phi}].$$

- Equation 19.41: Changed for compatibility with earlier definition of reward:

$$\boldsymbol{\theta} \leftarrow \boldsymbol{\theta} + \alpha \cdot \frac{1}{I}\sum_{i=1}^{I}\sum_{t=1}^{T} \frac{\partial \log\bigl[Pr(a_{it}|\mathbf{s}_{it}, \boldsymbol{\theta})\bigr]}{\partial \boldsymbol{\theta}} \Bigl(r_{i,t+1} + \gamma \cdot v[\mathbf{s}_{i,t+1}, \boldsymbol{\phi}] - v[\mathbf{s}_{i,t}, \boldsymbol{\phi}]\Bigr).$$

- Equation 19.42: Changed for compatibility with earlier definition of reward:

$$L[\boldsymbol{\phi}] = \sum_{i=1}^{I}\sum_{t=1}^{T}\left(r_{i,t+1} + \gamma \cdot v[\mathbf{s}_{i,t+1}, \boldsymbol{\phi}] - v[\mathbf{s}_{i,t}, \boldsymbol{\phi}]\right)^2.$$

- Figure 19.18 Legend. One trajectory through an ~~MDP~~ MRP

- Problem 19.1 Figure 19.18 shows a single trajectory through ~~the example MDP~~ an example MRP

- Problem 19.3 Added clarification that discount value is 0.9

- Section 20.12 if each of the 40 inputs of the MNIST-1D data were quantized into 10 possible values, there would be $10^{40}$ possible inputs, which is a factor of ~~$10^{35}$~~ $10^{36}$ more than the number of training examples.

- Section 20.12 A fully connected network for MNIST-1D with two hidden layers of width 400 can create mappings with up to $10^{42}$ linear regions. That's roughly ~~$10^{37}$~~ $10^{38}$ regions per training example, so very few of these regions contain data at any stage during training;

- Figure 21.1 Caption Structural description of the value alignment problem. ~~a)~~ Problems arise from a) misaligned objectives (e.g., bias) or b) informational asymmetries between a (human) principal and an (artificial) agent (e.g., lack of explainability).

- Section B.3.2 Minor clarification: For a vector $\mathbf{z}$, the $\ell_p$ norm is defined as:

$$||\mathbf{z}||_p = \left(\sum_{d=1}^{D} |z_d|^p\right)^{1/p}, \tag{1.13}$$

  for real-valued $p > 1$.

- Section C.2.1 Added missing equation numbers

- Section C.3.3 Added missing equation number

- Figure C.4 When the covariance matrix is a multiple of the ~~diagonal~~ identity matrix, the isocontours are circles, and we refer to this as spherical covariance.

- Section C.4.2. Consider a joint distribution $Pr(x, y, z)$ over three variables, $x, y$, and $z$, which in this particular case factors as:

## Second and third printings (Mar 2024)

These are things that are wrong and need to be fixed, but that will probably not affect your understanding (e.g., math symbols that are in bold but should not be).

- Section 1.1: ...and what is meant by "training" a model.
- Figure 1.13: ~~Adapted from Pablok (2017).~~
- Figure 2.3 legend: Each combination of parameters $\boldsymbol{\phi} = [\phi_0, \phi_1]^T$.
- Section 2.3: 1D linear regression has the obvious drawback
- Figure 3.5 legend: The universal approximation theorem proves that, with enough hidden units, there exists a shallow neural network that can describe any given continuous function defined on a compact subset of $\mathbb{R}^{D_i}$ to arbitrary precision.
- Notes page 38 Most of these are attempts to avoid the dying ReLU problem while limiting the gradient for negative values.
- Figure 4.1 legend: The first network maps inputs $x \in [-1, 1]$ to outputs $y \in [-1, 1]$ using a function comprising three linear regions that are chosen so that they alternate the sign of their slope (fourth linear region is outside range of graph).
- Figure 4.2: Colors changed to avoid ambiguity
- Equation 4.13 is missing a prime sign:

$$\begin{aligned} \mathbf{h} &= \mathbf{a}[\boldsymbol{\theta}_0 + \boldsymbol{\theta}x] \\ \mathbf{h}' &= \mathbf{a}[\boldsymbol{\psi}_0 + \boldsymbol{\Psi}\mathbf{h}] \\ y' &= \phi'_0 + \boldsymbol{\phi}'\mathbf{h}', \end{aligned}$$

- Equation 4.14: $\phi'_0$ should not be bold.

$$y = \phi'_0 + \boldsymbol{\phi}'\mathbf{h}'$$

- Equation 4.17 is not technically wrong, but the product is unnecessary and it's unclear if the last term should be included in it (no). Better written as:

$$N_r = \left(\frac{D}{D_i} + 1\right)^{D_i(K-1)} \cdot \sum_{j=0}^{D_i} \binom{D}{j}.$$

- Equation 5.10. Second line is disambiguated by adding brackets:

$$\begin{aligned}\hat{\boldsymbol{\phi}} &= \underset{\boldsymbol{\phi}}{\operatorname{argmin}}\left[-\sum_{i=1}^{I}\log\left[\frac{1}{\sqrt{2\pi\sigma^2}}\exp\left[-\frac{(y_i-\mathrm{f}[\mathbf{x}_i,\boldsymbol{\phi}])^2}{2\sigma^2}\right]\right]\right]\\ &= \underset{\boldsymbol{\phi}}{\operatorname{argmin}}\left[-\sum_{i=1}^{I}\left(\log\left[\frac{1}{\sqrt{2\pi\sigma^2}}\right]-\frac{(y_i-\mathrm{f}[\mathbf{x}_i,\boldsymbol{\phi}])^2}{2\sigma^2}\right)\right]\\ &= \underset{\boldsymbol{\phi}}{\operatorname{argmin}}\left[-\sum_{i=1}^{I}-\frac{(y_i-\mathrm{f}[\mathbf{x}_i,\boldsymbol{\phi}])^2}{2\sigma^2}\right]\\ &= \underset{\boldsymbol{\phi}}{\operatorname{argmin}}\left[\sum_{i=1}^{I}(y_i-\mathrm{f}[\mathbf{x}_i,\boldsymbol{\phi}])^2\right],\end{aligned}$$

- Equation 5.12. More properly written as:

$$\hat{y} = \underset{y}{\operatorname{argmax}}\left[Pr(y|\mathrm{f}[\mathbf{x},\hat{\boldsymbol{\phi}},\sigma^2])\right]. \tag{1.14}$$

  although the value of $\sigma^2$ does not actually matter or change the position of the maximum.

- Equation 5.15. Disambiguated by adding brackets:

$$\hat{\boldsymbol{\phi}} = \underset{\boldsymbol{\phi}}{\operatorname{argmin}}\left[-\sum_{i=1}^{I}\left(\log\left[\frac{1}{\sqrt{2\pi\mathrm{f}_2[\mathbf{x}_i,\boldsymbol{\phi}]^2}}\right]-\frac{(y_i-\mathrm{f}_1[\mathbf{x}_i,\boldsymbol{\phi}])^2}{2\mathrm{f}_2[\mathbf{x}_i,\boldsymbol{\phi}]^2}\right)\right].$$

- Section 5.5 The likelihood that input $\mathbf{x}$ has label $y=k$ (figure 5.10) is hence:

- Section 5.6 Removed $i$ index from this paragraph for consistency. Independence implies that we treat the probability $Pr(\mathbf{y}|\mathbf{f}[\mathbf{x},\boldsymbol{\phi}])$ as a product of univariate terms for each element $y_d \in \mathbf{y}$:

$$Pr(\mathbf{y}|\mathbf{f}[\mathbf{x},\boldsymbol{\phi}]) = \prod_d Pr(y_d|\mathbf{f}_d[\mathbf{x},\boldsymbol{\phi}]),$$

  where $\mathbf{f}_d[\mathbf{x},\boldsymbol{\phi}]$ is the $d^{th}$ set of network outputs, which describe the parameters of the distribution over $y_d$. For example, to predict multiple continuous variables $y_d \in \mathbb{R}$, we use a normal distribution for each $y_d$, and the network outputs $\mathrm{f}_d[\mathbf{x},\boldsymbol{\phi}]$ predict the means of these distributions. To predict multiple discrete variables $y_d \in \{1,2,\ldots,K\}$, we use a categorical distribution for each $y_d$. Here, each set of network outputs $\mathbf{f}_d[\mathbf{x},\boldsymbol{\phi}]$ predicts the $K$ values that contribute to the categorical distribution for $y_d$.

- Problem 5.8. Construct a loss function for making multivariate predictions $\mathbf{y}\in\mathbb{R}^{D_i}$ based on independent normal distributions…

- Notes page 94. However, this is strange since SGD is a special case of Adam (when $\beta = \gamma = 0$)
- Section 7.3. The final derivatives from the term $f_0 = \beta_0 + \omega_0 \cdot x_i$ are:
- Section 7.4. Similarly, the derivative for the weights matrix $\mathbf{\Omega}_k$, is given by
- Section 7.5.1 and the second moment $\mathbb{E}[h_j^2]$ will be half the variance $\sigma_f^2$
- Figure 7.8. Not wrong, but changed to "nn.init.kaiming_normal_(layer_in.weight)" for compatability with text and to avoid deprecated warning.
- Section 8.3.3 (i.e., with four hidden units and four linear regions in the range of the data) + minor changes in text to accommodate extra words
- Figure 8.9 number of hidden units / linear regions in range of data
- Section 8.4.1 When the number of parameters is very close to the number of training data examples (figure 8.11b)
- Figure 9.5 legend: Effect of learning rate (LR) and batch size for 4000 training and 4000 test examples from MNIST-1D (see figure 8.1) for a neural network with two hidden layers. a) Performance is better for large learning rates than for intermediate or small ones. In each case, the number of iterations is 6000/LR, so each solution has the opportunity to move the same distance.
- Figure 10.3. The dilation rates are wrong by one, so should be 1,1,1, and 2 in panels a,b,c,d, respectively.
- Section 10.2.1 Not wrong, but could be disambiguated: The size of the region over which inputs are combined is termed the *kernel size*.
- Section 10.2.3 The number of zeros we intersperse between the weights determines the dilation rate.
- Section 10.2.4 With kernel size three, stride one, and dilation rate one.
- Section 10.2.7 The convolutional network has 2,050 parameters, and the fully connected network has 59,065 parameters.
- Figure 10.8 Number of parameters also wrong in figure 10.8 (correct version in this document). Recalculated curve is slightly different.
- Section 10.5.3 The first part of the network is a smaller version of VGG (figure 10.17) that contains thirteen rather than sixteen convolutional layers.
- Section 10.6 The weights and the bias are the same at every spatial position, so there are far fewer parameters than in a fully connected network, and the number of parameters doesn't increase with the input image size.

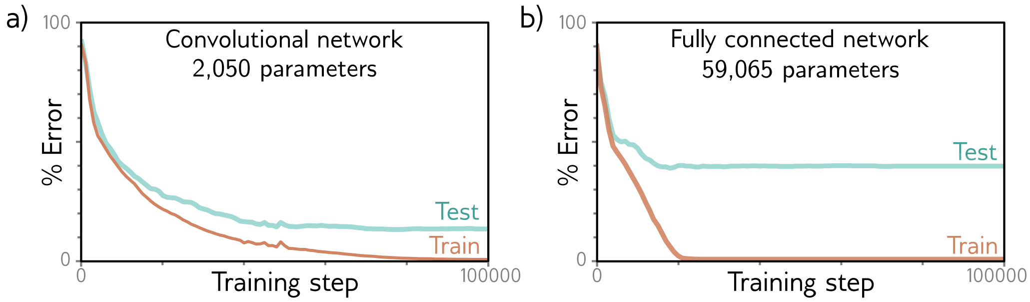


Corrected version of figure 10.8

- Problem 10.1 Show that the operation in equation 10.3 is equivariant with respect to translation.
- Problem 10.2 Equation 10.3 defines 1D convolution with a kernel size of three, stride of one, and dilation one.
- Problem 10.3 Write out the equation for the 1D dilated convolution with a kernel size of three and a dilation rate of two.
- Problem 10.4 Write out the equation for a 1D convolution with kernel size of seven, a dilation rate of three, and a stride of three.
- Problem 10.9 A network consists of three 1D convolutional layers. At each layer, a zero-padded convolution with kernel size three, stride one, and dilation one is applied.
- Problem 10.10 A network consists of three 1D convolutional layers. At each layer, a zero-padded convolution with kernel size seven, stride one, and dilation one is applied.
- Problem 10.11 Consider a convolutional network with 1D input $\mathbf{x}$. The first hidden layer $\mathbf{H}_1$ is computed using a convolution with kernel size five, stride two, and a dilation rate of one. The second hidden layer $\mathbf{H}_2$ is computed using a convolution with kernel size three, stride one, and a dilation rate of one. The third hidden layer $\mathbf{H}_3$ is computed using a convolution with kernel size five, stride one, and a dilation rate of two. What are the receptive field sizes at each hidden layer?
- Legend to figure 11.15. Computational graph for batch normalization (see problem 11.5).
- Section 12.2: Not a mistake, but this is clearer: where $\boldsymbol{\beta}_v \in \mathbb{R}^D \times 1$ and $\boldsymbol{\Omega}_v \in \mathbb{R}^{D\times D}$ represent biases and weights, respectively.
- Section 12.3.3 to make self-attention work well
- Section 12.4 Title changed to Transformer layers
- Section 12.4 a larger transformer mechanism

- Section 12.4 a series of these transformer layers ...
- Section 12.5 The previous section described the transformer layer... a series of transformer layers...
- Figure 12.8 legend: The transformer → Transformer layer...The transformer layer consists
- Figure 12.8 has some minor mistakes in the calculation. The corrected version is shown at the end of this document.
- Figure 12.8 legend. At each iteration, the sub-word tokenizer looks for the most commonly occurring adjacent pair of tokens
- Section 12.5.3 a series of $K$ transformer layers
- Section 12.6 through 24 transformer layers
- Section 12.6 in the fully connected networks ~~in the transformer~~ is 4096
- Figure 12.10 legend: a series of transformer layers
- Section 12.7.2 the transformer layers use masked...
- Figure 12.12 are passed through a series of transformer layers... and those of tokens earlier
- Section 12.7.4 There are 96 transformer layers
- Section 12.7 comprises a series of transformer layers
- Section 12.8 Originally, these
- Section 12.8 a series of transformer layers... a series of transformer layers
- Section 13.5.1 Given $I$ training graphs $\{\mathbf{X}_i, \mathbf{A}_i\}$ and their labels $y_i$, the parameters $\boldsymbol{\Phi} = \{\boldsymbol{\beta}_k, \boldsymbol{\Omega}_k\}_{k=0}^{K}$ can be learned using SGD...
- Figure 15.3 legend: At the end is a tanh function that maps the...
- Figure 15.3 arctan → tanh. Corrected version nearby in this document.
- Section 15.1.3: At the final layer, the 64×64×3 signal is passed through a tanh function to generate an image $\mathbf{x}^*$
- Equation 15.6. Minor problems with brackets in this equation. Should be:

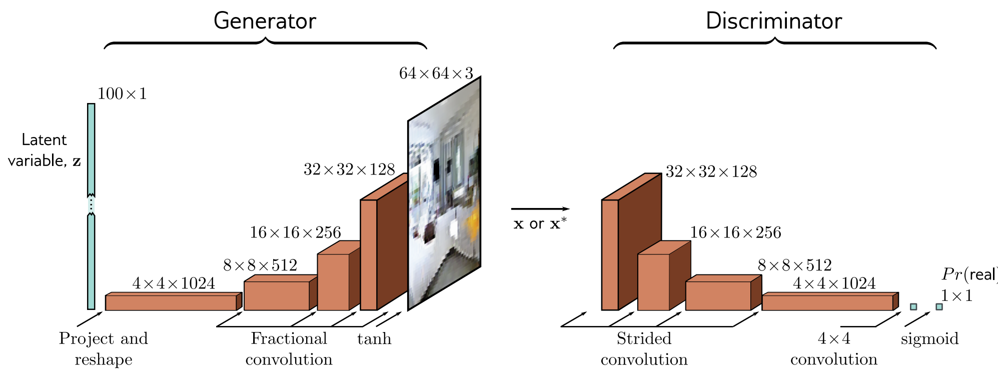


Corrected version of figure 15.3

$$
\begin{aligned}
L[\boldsymbol{\phi}] &= \frac{1}{J}\sum_{j=1}^{J}\left(\log\left[1-\text{sig}[\text{f}[\mathbf{x}_j^*,\boldsymbol{\phi}]]\right]\right)+\frac{1}{I}\sum_{i=1}^{I}\left(\log\left[\text{sig}[\text{f}[\mathbf{x}_i,\boldsymbol{\phi}]]\right]\right)\\
&\approx \mathbb{E}_{\mathbf{x}^*}\left[\log\left[1-\text{sig}[\text{f}[\mathbf{x}^*,\boldsymbol{\phi}]]\right]\right]+\mathbb{E}_{\mathbf{x}}\left[\log\left[\text{sig}[\text{f}[\mathbf{x},\boldsymbol{\phi}]]\right]\right]\\
&= \int Pr(\mathbf{x}^*)\log\left[1-\text{sig}[\text{f}[\mathbf{x}^*,\boldsymbol{\phi}]]\right]d\mathbf{x}^*+\int Pr(\mathbf{x})\log\left[\text{sig}[\text{f}[\mathbf{x},\boldsymbol{\phi}]]\right]d\mathbf{x}.
\end{aligned}
$$

- Equation 16.2 (last line). For some reason, this didn't print properly, although it looks fine in my original pdf. Should be:

$$
\begin{aligned}
\hat{\boldsymbol{\phi}} &= \underset{\boldsymbol{\phi}}{\text{argmax}}\left[\prod_{i=1}^{I}Pr(x_i|\boldsymbol{\phi})\right]\\
&= \underset{\boldsymbol{\phi}}{\text{argmin}}\left[\sum_{i=1}^{I}-\log\left[Pr(x_i|\boldsymbol{\phi})\right]\right]\\
&= \underset{\boldsymbol{\phi}}{\text{argmin}}\left[\sum_{i=1}^{I}\log\left[\left|\frac{\partial\text{f}[z_i,\boldsymbol{\phi}]}{\partial z_i}\right|\right]-\log\left[Pr(z_i)\right]\right],
\end{aligned}
$$

- Equation 16.25. $\boldsymbol{\phi}$ should change to $\hat{\boldsymbol{\phi}}$ on left hand side. Correct version is:

$$
\hat{\boldsymbol{\phi}} = \underset{\boldsymbol{\phi}}{\text{argmin}}\left[\text{KL}\left[\sum_{i=1}^{I}\delta\left[\mathbf{x}-\text{f}[\mathbf{z}_i,\boldsymbol{\phi}]\right]\middle|\middle|q(\mathbf{x})\right]\right].
$$

- Equation 16.26. $\boldsymbol{\phi}$ should change to $\hat{\boldsymbol{\phi}}$ on left hand side. Correct version is:

$$
\hat{\boldsymbol{\phi}} = \underset{\boldsymbol{\phi}}{\text{argmin}}\left[\text{KL}\left[\frac{1}{I}\sum_{i=1}^{I}\delta[\mathbf{x}-\mathbf{x}_i]\middle|\middle|Pr(\mathbf{x}_i,\boldsymbol{\phi})\right]\right].
$$

- Equation 18.24 has a minor formatting mistake. Better written as:

$$
\begin{aligned}
\log\left[\frac{Pr(\mathbf{x},\mathbf{z}_{1\ldots T}|\boldsymbol{\phi}_{1\ldots T})}{q(\mathbf{z}_{1\ldots T}|\mathbf{x})}\right] & \\
&= \log\left[\frac{Pr(\mathbf{x}|\mathbf{z}_1,\boldsymbol{\phi}_1)}{q(\mathbf{z}_1|\mathbf{x})}\right] + \log\left[\frac{\prod_{t=2}^{T} Pr(\mathbf{z}_{t-1}|\mathbf{z}_t,\boldsymbol{\phi}_t)\cdot q(\mathbf{z}_{t-1}|\mathbf{x})}{\prod_{t=2}^{T} q(\mathbf{z}_{t-1}|\mathbf{z}_t,\mathbf{x})\cdot q(\mathbf{z}_t|\mathbf{x})}\right] + \log\Big[Pr(\mathbf{z}_T)\Big]\\
&= \log\left[Pr(\mathbf{x}|\mathbf{z}_1,\boldsymbol{\phi}_1)\right] + \log\left[\frac{\prod_{t=2}^{T} Pr(\mathbf{z}_{t-1}|\mathbf{z}_t,\boldsymbol{\phi}_t)}{\prod_{t=2}^{T} q(\mathbf{z}_{t-1}|\mathbf{z}_t,\mathbf{x})}\right] + \log\left[\frac{Pr(\mathbf{z}_T)}{q(\mathbf{z}_T|\mathbf{x})}\right]\\
&\approx \log\left[Pr(\mathbf{x}|\mathbf{z}_1,\boldsymbol{\phi}_1)\right] + \sum_{t=2}^{T}\log\left[\frac{Pr(\mathbf{z}_{t-1}|\mathbf{z}_t,\boldsymbol{\phi}_t)}{q(\mathbf{z}_{t-1}|\mathbf{z}_t,\mathbf{x})}\right],
\end{aligned}
$$

- Equation 18.34 missing indices on noise term:

$$
\begin{aligned}
L[\boldsymbol{\phi}_{1\ldots T}] &= \sum_{i=1}^{I} -\log\Big[\text{Norm}_{\mathbf{x}_i}\left[\mathbf{f}_1[\mathbf{z}_{i1},\boldsymbol{\phi}_1],\sigma_1^2\mathbf{I}\right]\Big] \qquad (1.15)\\
&+\sum_{t=2}^{T}\frac{1}{2\sigma_t^2}\left\|\left(\frac{1}{\sqrt{1-\beta_t}}\mathbf{z}_{it}-\frac{\beta_t}{\sqrt{1-\alpha_t}\sqrt{1-\beta_t}}\boldsymbol{\epsilon}_{it}\right)-\mathbf{f}_t[\mathbf{z}_{it},\boldsymbol{\phi}_t]\right\|^2.
\end{aligned}
$$

- Section 20.2.2 Another possible explanation for the ease with which models are trained is that some regularization methods like L2 regularization (weight decay) make the loss surface flatter and more convex.

- Section 20.2.4 For example, Du et al. (2019a) show that residual networks converge to zero training loss when the width of the network $D$ (i.e., the number of hidden units) is $\Omega[I^4K^2]$ where $I$ is the amount of training data, and $K$ is the depth of the network.

- Section 21.7 the Conference on AI, Ethics, and Society

- Appendix A. The notation $\{0,1,2,\ldots\}$ denotes the set of non-negative integers.

- Appendix A ...*big-O* notation, which represents an upper bound...

- Appendix A. $\text{f}[n] < c\cdot\text{g}[n]$ for all $n > n_0$

- Equation B. 18

$$
\begin{aligned}
y_1 &= \phi_{10}+\phi_{11}z_1+\phi_{12}z_2+\phi_{13}z_3\\
y_2 &= \phi_{20}+\phi_{21}z_1+\phi_{22}z_2+\phi_{23}z_3\\
y_3 &= \phi_{30}+\phi_{31}z_1+\phi_{32}z_2+\phi_{33}z_3. \qquad (1.16)
\end{aligned}
$$

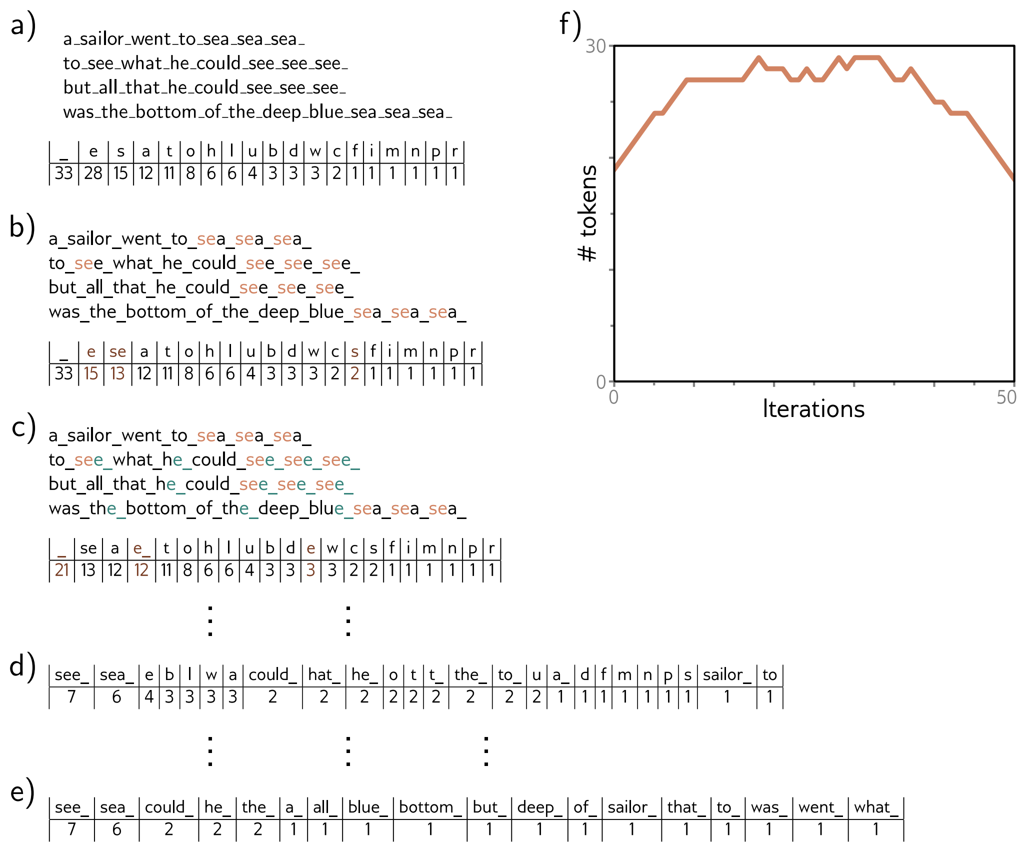


Corrected version of figure 12.8

- Appendix C.5.4 Accent in wrong place: The Fréchet and Wasserstein distances...
- Equation C.32.

$$D_{KL}\Bigl[\text{Norm}[\boldsymbol{\mu}_1,\boldsymbol{\Sigma}_1]\Bigl|\Bigr|\text{Norm}[\boldsymbol{\mu}_2,\boldsymbol{\Sigma}_2]\Bigr] = \frac{1}{2}\left(\log\left[\frac{|\boldsymbol{\Sigma}_2|}{|\boldsymbol{\Sigma}_1|}\right] - D + \text{tr}\left[\boldsymbol{\Sigma}_2^{-1}\boldsymbol{\Sigma}_1\right] + (\boldsymbol{\mu}_2-\boldsymbol{\mu}_1)\boldsymbol{\Sigma}_2^{-1}(\boldsymbol{\mu}_2-\boldsymbol{\mu}_1)\right]\Bigr).$$

## First printing (Dec 2023)

These are things that are wrong and need to be fixed, but that will probably not affect your understanding (e.g., math symbols that are in bold but should not be).

- Section 1.1.1: In contrast, the model in figure 1.2b takes the chemical structure of a molecule as an input and predicts both the freezing and boiling points.
- Figure 1.2 legend: This *multivariate regression* model takes the structure of a chemical molecule and predicts its freezing and boiling points.
- Section 1.1.2: Finally, consider the input for the model that predicts the freezing and boiling points of the molecule. A molecule may contain varying numbers of atoms that can
- Multiple places in Chapters 2-9. Loss functions $L[\boldsymbol{\phi}]$ sometimes written as $\mathrm{L}[\boldsymbol{\phi}]$. Have now all been converted to italic for consistency.
- Section 3.1.1 The slope of each linear region is determined by ~~(i)~~ the original slopes $\theta_{\bullet 1}$ of the active inputs for this region and ~~(ii)~~ the weights $\phi_{\bullet}$ that were subsequently applied.
- Section 4.5.5 Added missing definition of over-parameterization and other minor changes for typesetting consistence: It may be that over-parameterized deep models (i.e., those with more parameters than training examples) have a large family...
- Chapter 4 Notes, page 52. Montúfar
- Problem 4.7: Choose values for the parameters $\boldsymbol{\phi} = \{\phi_0, \phi_1, \phi_2, \phi_3, \theta_{10}, \theta_{11}, \theta_{20}, \theta_{21}, \theta_{30}, \theta_{31}\}$ for the shallow neural network in equation 3.1 (with ReLU activation functions) that will define an identity function over a finite range $x \in [a, b]$.
- Problem 4.11: How many parameters does each network have? How many linear regions can each network make (see equation 4.17)?
- Problem 5.1 Reworded to be more precise with limits: Show that the logistic sigmoid function $\text{sig}[z]$ becomes 0 as $z \to -\infty$, is 0.5 when $z = 0$, and becomes 1 when $z \to \infty$.
- Problem 5.3: The term $\text{Bessel}_0[\kappa]$ is a modified Bessel function of the first kind of order 0.
- Problem 5.8: Construct a loss function for making multivariate predictions $\mathbf{y} \in \mathbb{R}^{D_o}$ based on...
- Figure 7.4 legend: We work backward from the end of the function computing the derivatives $\partial \ell_i / \partial f_k$ and $\partial \ell_i / \partial h_k$ of the loss with respect to the intermediate quantities.
- Section 7.3 Finally, we consider how the loss $\ell_i$ changes when we change the parameters $\{\beta_k\}$ and $\{\omega_k\}$.
- Figure 7.5 legend: Finally, we compute the derivatives $\partial \ell_i / \partial \beta_k$ and $\partial \ell_i / \partial \omega_k$
- Problem 7.13 For the same function as in problem 7.12, compute the derivative...

- Equation 8.2:

$$
\begin{aligned}
L[x] &= \big(\mathrm{f}[x,\boldsymbol{\phi}] - y[x]\big)^2 \qquad (1.17) \\
&= \Big(\big(\mathrm{f}[x,\boldsymbol{\phi}] - \mu[x]\big) + \big(\mu[x] - y[x]\big)\Big)^2 \\
&= \big(\mathrm{f}[x,\boldsymbol{\phi}] - \mu[x]\big)^2 + 2\big(\mathrm{f}[x,\boldsymbol{\phi}]\cancel{)} - \mu[x]\big)\big(\mu[x] - y[x]\big) + \big(\mu[x] - y[x]\big)^2,
\end{aligned}
$$

- Section 8.4.1 There would be $10^{40}$ bins in total, constrained by only $10^4$ examples.
- Equation 9.6 LHS should be total derivative, not partial derivative:

$$\frac{d\boldsymbol{\phi}}{dt} = -\frac{\partial L}{\partial \boldsymbol{\phi}}. \qquad (1.18)$$

- Figure 9.4 Added to legend for panel (a) Blue point represents global minimum. Added to legend for panel (d) Blue point represents global minimum which may now be in a different place from panel (a).
- Figure 9.9 legend Here we are using full-batch gradient descent, and the model (from figure 8.4) fits the data as well as possible, so further training won't remove the kink
- Figure 9.9 legend Consider what happens if we remove the eighth hidden unit
- Figure 9.11 legend: a-c) Two sets of parameters (cyan and gray curves) sampled from the posterior
- Figure 9.11 legend When the prior variance $\sigma^2_{\phi}$ is small
- Equation 9.15 Should be total derivative not partial:

$$\frac{d\boldsymbol{\phi}}{dt} = \mathbf{g}[\boldsymbol{\phi}]. \qquad (1.19)$$

- Equation 9.16 Should be total derivative not partial:

$$\frac{d\boldsymbol{\phi}}{dt} \approx \mathbf{g}[\boldsymbol{\phi}] + \alpha\mathbf{g}_1[\boldsymbol{\phi}] + \ldots, \qquad (1.20)$$

- Equation 9.17 Should be total derivative not partial:

$$
\begin{aligned}
\boldsymbol{\phi}[\alpha] &\approx \boldsymbol{\phi} + \alpha\frac{d\boldsymbol{\phi}}{dt} + \frac{\alpha^2}{2}\frac{d^2\boldsymbol{\phi}}{dt^2}\bigg|_{\boldsymbol{\phi}=\boldsymbol{\phi}_0} \\
&\approx \boldsymbol{\phi} + \alpha\left(\mathbf{g}[\boldsymbol{\phi}] + \alpha\mathbf{g}_1[\boldsymbol{\phi}]\right) + \frac{\alpha^2}{2}\left(\frac{\partial\mathbf{g}[\boldsymbol{\phi}]}{\partial\boldsymbol{\phi}}\frac{d\boldsymbol{\phi}}{dt} + \alpha\frac{\partial\mathbf{g}_1[\boldsymbol{\phi}]}{\partial\boldsymbol{\phi}}\frac{d\boldsymbol{\phi}}{dt}\right)\bigg|_{\boldsymbol{\phi}=\boldsymbol{\phi}_0} \\
&= \boldsymbol{\phi} + \alpha\left(\mathbf{g}[\boldsymbol{\phi}] + \alpha\mathbf{g}_1[\boldsymbol{\phi}]\right) + \frac{\alpha^2}{2}\left(\frac{\partial\mathbf{g}[\boldsymbol{\phi}]}{\partial\boldsymbol{\phi}}\mathbf{g}[\boldsymbol{\phi}] + \alpha\frac{\partial\mathbf{g}_1[\boldsymbol{\phi}]}{\partial\boldsymbol{\phi}}\mathbf{g}[\boldsymbol{\phi}]\right)\bigg|_{\boldsymbol{\phi}=\boldsymbol{\phi}_0} \\
&\approx \boldsymbol{\phi} + \alpha\mathbf{g}[\boldsymbol{\phi}] + \alpha^2\left(\mathbf{g}_1[\boldsymbol{\phi}] + \frac{1}{2}\frac{\partial\mathbf{g}[\boldsymbol{\phi}]}{\partial\boldsymbol{\phi}}\mathbf{g}[\boldsymbol{\phi}]\right)\bigg|_{\boldsymbol{\phi}=\boldsymbol{\phi}_0}, \qquad (1.21)
\end{aligned}
$$

- Equation 9.19 Should be total derivative not partial:

$$\begin{aligned}\frac{d\boldsymbol{\phi}}{dt} &\approx \mathbf{g}[\boldsymbol{\phi}] + \alpha\mathbf{g}_1[\boldsymbol{\phi}] \\ &= -\frac{\partial L}{\partial \boldsymbol{\phi}} - \frac{\alpha}{2}\left(\frac{\partial^2 L}{\partial \boldsymbol{\phi}^2}\right)\frac{\partial L}{\partial \boldsymbol{\phi}}. \end{aligned} \tag{1.22}$$

- Page 156 Notes: Wrong marginal reference — Appendix B.3.7 Spectral Norm
- Figure 10.3 legend – In dilated or atrous convolution (from the French "à trous" – with holes), we intersperse zeros in the weight vector...
- Section 10.5.1 A final max-pooling layer yields a 6×6 representation with 256 channels which is resized into a vector of length 9, 216 and passed through three fully connected layers containing 4096, 4096, and 1000 hidden units, respectively.
- Section 10.5.1 The complete network contains ∼60 million parameters, most of which are in the fully connected layers ~~and the end of the network~~.
- Problem 10.4 Write out the equation for a 1D convolution with kernel size of seven, a dilation rate of three, and a stride of three. You may assume that the input is padded with zeros at positions $x_{-2}$, $x_{-1}$ and $x_0$.
- Equation 11.3: Terms should be reordered to be consistent with definition of vector derivative in appendix:

$$\frac{\partial \mathbf{y}}{\partial \mathbf{f}_1} = \frac{\partial \mathbf{f}_2}{\partial \mathbf{f}_1}\frac{\partial \mathbf{f}_3}{\partial \mathbf{f}_2}\frac{\partial \mathbf{f}_4}{\partial \mathbf{f}_3}. \tag{1.23}$$

- Equation 11.6: Terms should be reordered to be consistent with definition of vector derivative in appendix:

$$\frac{\partial \mathbf{y}}{\partial \mathbf{f}_1} = \mathbf{I} + \frac{\partial \mathbf{f}_2}{\partial \mathbf{f}_1} + \left(\frac{\partial \mathbf{f}_3}{\partial \mathbf{f}_1} + \frac{\partial \mathbf{f}_2}{\partial \mathbf{f}_1}\frac{\partial \mathbf{f}_3}{\partial \mathbf{f}_2}\right) + \left(\frac{\partial \mathbf{f}_4}{\partial \mathbf{f}_1} + \frac{\partial \mathbf{f}_2}{\partial \mathbf{f}_1}\frac{\partial \mathbf{f}_4}{\partial \mathbf{f}_2} + \frac{\partial \mathbf{f}_3}{\partial \mathbf{f}_1}\frac{\partial \mathbf{f}_4}{\partial \mathbf{f}_3} + \frac{\partial \mathbf{f}_2}{\partial \mathbf{f}_1}\frac{\partial \mathbf{f}_3}{\partial \mathbf{f}_2}\frac{\partial \mathbf{f}_4}{\partial \mathbf{f}_3}\right), \tag{1.24}$$

- Equation 11.10:

$$\begin{aligned} f_1 &= \mathbb{E}[z_i] & f_5 &= \sqrt{f_4 + \epsilon} \\ f_{2i} &= z_i - f_1 & f_6 &= 1/f_5 \\ f_{3i} &= f_{2i}^2 & f_{7i} &= f_{2i} \times f_6 \\ f_4 &= \mathbb{E}[f_{3i}] & z_i' &= f_{7i} \times \gamma + \delta, \end{aligned} \tag{1.25}$$

- Figure 12.10 legend: A small fraction of the input tokens are randomly replaced with...
- Section 12.2.1 Not technically wrong, but for consistency with previous and following sections: Equation 12.2 shows that the same weights $\boldsymbol{\Omega}_v \in \mathbb{R}^{D\times D}$ and biases $\boldsymbol{\beta}_v \in \mathbb{R}^D$ are applied to each input $\mathbf{x}_{\bullet} \in \mathbb{R}^D$...

- Section 12.2.1 Not technically, wrong, but for consistency with previous and following sections: It follows that the number of attention weights has a quadratic dependence on the sequence length $N$, but is independent of the length $D$ of each input $\mathbf{x}_{\bullet}$.

- Section 12.3.1 Each element of the attention matrix corresponds to a particular offset between key position $a$ and query position $b$.

- Section 12.3.2 title: Scaled dot-product self-attention

- Section 12.3.2 This is known as *scaled dot-product self-attention*.

- Problem 12.1 How many weights and biases would there be in a fully connected shallow network relating all $DN$ inputs to all $DN$ outputs?

- Notes Page 236 Much subsequent work has modified just the attention matrix so that in the scaled dot-product self-attention equation:

- Problem 12.10: Extra bracket removed:

$$a[\mathbf{x}_m, \mathbf{x}_n] = \text{softmax}_m\left[\mathbf{k}_\bullet^T \mathbf{q}_n\right] = \frac{\exp\left[\mathbf{k}_m^T \mathbf{q}_n\right]}{\sum_{m'=1}^{N} \exp\left[\mathbf{k}_{m'}^T \mathbf{q}_n\right]}. \tag{1.26}$$

- Figure 13.10 Right hand column should be labelled as "output" not "hidden layer two". item Equation 13.22

$$\mathbf{H}'_k = \boldsymbol{\beta}_k \mathbf{1}^T + \boldsymbol{\Omega}_k \mathbf{H}_k. \tag{1.27}$$

- Section 15.1 A single new sample $\mathbf{x}_j^*$ is generated by (i) choosing a *latent variable* $\mathbf{z}_j$ from a simple base distribution (e.g., a standard normal) and then (ii) passing this data through a network $\mathbf{x}_j{}^* = \mathbf{g}[\mathbf{z}_j, \boldsymbol{\theta}]$ with parameters $\boldsymbol{\theta}$

- Section 15.2.1 If we divide the two sums in the first line of equation 15.5 by the numbers...

- Section 15.2.1 When $I = J$, the optimal discriminator for an example $\tilde{\mathbf{x}}$ of unknown origin is:

- Equation 16.12:

$$\text{f}[h, \boldsymbol{\phi}] = \left(\sum_{k=1}^{b-1} \phi_k\right) + (hK - b)\phi_b, \tag{1.28}$$

- Equation 16.25:

$$\hat{\boldsymbol{\phi}} = \underset{\boldsymbol{\phi}}{\text{argmin}}\left[\text{KL}\left[\frac{1}{I}\sum_{i=1}^{I} \delta\left[\mathbf{x} - \text{f}[\mathbf{z}_i, \boldsymbol{\phi}]\right]\middle\|\, q(\mathbf{x})\right]\right]. \tag{1.29}$$

- Section 16.2 The first term is the inverse of the determinant of the $D \times D$ Jacobian matrix $\partial\mathbf{f}[\mathbf{z}, \boldsymbol{\phi}]/\partial\mathbf{z}$, which contains elements $\partial\text{f}_i[\mathbf{z}, \boldsymbol{\phi}]/\partial z_j$ at position $(i, j)$.

- Section 17.5 we can't evaluate the evidence term $Pr(\mathbf{x}|\phi)$ in the denominator (see section 17.3).
- Equation 17.28 Brackets in third line now larger.
- Section 18.2 This is a *Markov chain* because the probability of $\mathbf{z}_t$ is determined entirely by the value of the immediately preceding variable $\mathbf{z}_{t-1}$.
- Section 18.6.1 The obvious architectural choice for this image-to-image mapping is the U-Net (figure 11.10).
- Section 19.7 Hence, the decision transformer replaces the reward $r_t$ with the *returns-to-go* $R_{t:T} = \sum_{t'=t}^{T} r_{t'}$ (i.e., the sum of the empirically observed future rewards).
- Section 19.1.2 Rephrased as ambiguous: A *Markov reward process* extends the Markov process to include a distribution $Pr(r_{t+1}|s_t)$ over the possible rewards $r_{t+1}$ received at the next time step, given that we are in state $s_t$.
- Section 20.5.1 In general, the smaller the model, the larger the proportion of weights that can... Note that this statement is only true for pure pruning methods, and not for lottery tickets where the pruned network is retrained from scratch, and so it has been removed.
- Section C.2.1 Rule 2:

$$\begin{aligned}\mathbb{E}\bigl[k \cdot \mathrm{f}[x]\bigr] &= \int k \cdot \mathrm{f}[x] Pr(x) dx \\ &= k \cdot \int \mathrm{f}[x] Pr(x) dx \\ &= k \cdot \mathbb{E}\bigl[\mathrm{f}[x]\bigr].\end{aligned}$$

- Section C.5.4 Reformulated to reflect the fact that the Fréchet/ and 2-Wasserstein distances are the same:

  The Fréchet/2-Wasserstein distance is given by:

$$D^2_{Fr/W_2}\Bigl[\mathrm{Norm}[\boldsymbol{\mu}_1, \boldsymbol{\Sigma}_1]\Bigl|\Bigr|\mathrm{Norm}[\boldsymbol{\mu}_2, \boldsymbol{\Sigma}_2]\Bigr] = |\boldsymbol{\mu}_1 - \boldsymbol{\mu}_2|^2 + \mathrm{tr}\left[\boldsymbol{\Sigma}_1 + \boldsymbol{\Sigma}_2 - 2\left(\boldsymbol{\Sigma}_1\boldsymbol{\Sigma}_2\right)^{1/2}\right]. \tag{1.30}$$